OVER-THE-AIR RF CONFORMANCE MEASUREMENTS ON 5G NR DEVICES

White paper | Version 01.00 | Reiner Stuhlfauth, Heinz Mellein

ROHDE&SCHWARZ
Make ideas real

CONTENTS

1 INTRODUCTION

For wireless communications systems, user device testing was originally based on conducted measurements. Even on component level, RF connectors were available for measuring metrics and characterizing RF performance. Such metrics can be divided into TX performance parameters such as power level, EVM quality or spectral emissions, and RX performance parameters such as receiver sensitivity and selectivity. Antenna implementation also plays a crucial role in overall performance.

Due to the increasing integration of chipsets and antennas and the use of higher frequencies in the millimeterwave range, the boundaries between chipset testing, RF testing and antenna characterization have become blurred. Highly integrated antennas no longer allow isolated testing of chipset and passive antenna components. In FR2, cable connectors are no longer feasible. Aspects like shrinking component sizes only produce minor effects. In contrast, there are major challenges related to costs and other problems such as path attenuation, RF matching between connectors and susceptibility of connected setups to bending. The main impetus for a paradigm change in the test setup was the introduction of directional antennas in UEs. As a result, beamforming is no longer a feature that is only found in base stations. A new measurement domain was created. Analogous to familiar time based metrics (e.g. power versus time), spectrum based metrics (e.g. spectrum emission mask) and code domain based metrics (e.g. code domain power), spatial domain based metrics are now important. Terms like spherical radiation pattern and spherical receiver characteristics have become commonplace in the T&M industry.

Measurement characteristics and requirements specified by standardization organizations like 3GPP have been updated accordingly. Conformance testing must ensure proper implementation and operation of applicable systems.

The objective of this paper is to discuss the technical background for over-the-air (OTA) testing. Focusing on UEs, the paper examines the requirements described in the technical specifications.

Chapter 2 contains an overview of antenna measurement key parameters. Chapter 3 provides a general overview of OTA test methods and setups. Due to the complexity of the technology, there is no “one fits all” approach and engineers must understand the underlying test metrics.

Chapter 4 discusses 3GPP OTA testing for UEs in both directions, along with the relevant transmitter and receiver test aspects, methods and setups.

This paper focuses on RF conformance aspects. Other OTA test aspects such as production test setups, radio resource management and OTA setups for multi-technology testing (e.g. location based services or coexistence aspects) are not covered.

2 OTA FUNDAMENTALS

2.1 Antenna parameters

Antennas play a pivotal role in wireless communications systems. Modern communications technologies use sophisticated methods such as antenna/hardware integration, active components and directional antenna radiation (also known as beamforming). Especially at higher frequencies such as the millimeterwave frequency range (FR2) in 5G NR, conducted DUT measurements are no longer feasible due to smaller antenna sizes, cable costs and setup complexity and vulnerability to bending or mismatching. We could even say there has been a paradigm change in test setups. Since the introduction of directional antennas, measurements must be performed in the spatial domain, making over-the-air connections the way to go. This chapter provides a concise overview of antenna parameters as a foundation for subsequent chapters.

The IEEE 145-2013 standard defines a general model with a gain and directivity flow chart for antenna parameters. Subsequent sections provide a detailed description of this reference model [Ref. 3].

Figure 1: IEEE antenna term definition

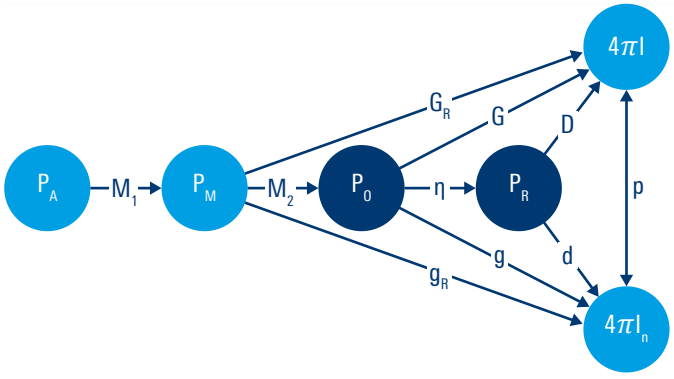

P_A: Power available from generator
P_M: Power to matched transmission line
P_0: Power accepted by antenna (feed power)
P_R: Power radiated by antenna
I: Radiation intensity (power flux)
η: Radiation efficiency
G_R: Realized gain
G: (Isotropic) gain
D: Directivity
M_1: Impedance mismatch 1
M_2: Impedance mismatch 2
I_n: Partial radiation intensity (i.e. per polarization)
g_R: Partial realized gain
g: Partial gain
d: Partial directivity
p: Polarization efficiency
EIRP: Equivalent isotropic radiated power

2.1.1 Antenna radiation model

The equations postulated by James Clerk Maxwell in 1864 were the initial milestone in the early history of antennas. He predicted the theoretical existence of electromagnetic waves. About 20 years later, it was Heinrich Hertz who demonstrated their real-world existence for the first time using a spark gap transmitter connected to an elementary antenna. The term Hertzian dipole is related to the theoretical model of an infinitely small dipole antenna used in these early experiments. From that point onwards, the science of radio waves progressed rapidly. By the beginning of the 20th century, Guglielmo Marconi was able to demonstrate radio signal transmission across the Atlantic Ocean.

The main responsibility of an antenna is to convert a conducted, cable based wave to a radiated wave propagating in free space (or vice versa). As we know, radiated waves are characterized by the magnetic field strength component H and the electric field strength component E. Under normal conditions, we assume orthogonality between E and H.

As a brief refresher, we will explore antenna fundamentals and discuss key parameters in antenna measurements. Electrical engineering explains “what” an antenna is, whereas physics explains “why” an antenna works. First, we can explore “why” an antenna radiates by looking at the electric field of any object, indicated by Coulomb’s law (the

magnetic field is just the cross-product of the electric field – so we only need one equation).

$$E = \frac{-q}{4\pi\varepsilon_0}\left[\frac{e_r}{r^2} + \frac{1}{c^2}\frac{d^2}{dt^2}e_r\right]$$

The Coulomb equation has two main parts. The first part is Coulomb's law for static (DC) fields. The lack of time dependency in electric fields dramatically simplifies Maxwell's equations, resulting in decoupled electric and magnetic fields (i.e. the electric field can be analyzed apart from the magnetic field).

The second part is radiation. **Radiation** is defined as the fields created by an accelerating electron. As one electron oscillates, the adjacent electrons in space also oscillate, thereby creating an outward wave. This means a field is created by electron movement on the wire. Assuming the example of a radiator as a dipole (see Figure 7), the maximum displacement is perpendicular to the wire. This is the direction of maximum radiation. In contrast, there is no perceived movement looking along the axis of the dipole, which results in zero radiation in the far field.

Finally, the radiated fields can be modulated (by phase, amplitude, "code", power, etc.) in order to transfer information – the goal of wireless communications.

Figure 2: Antenna and impedance model

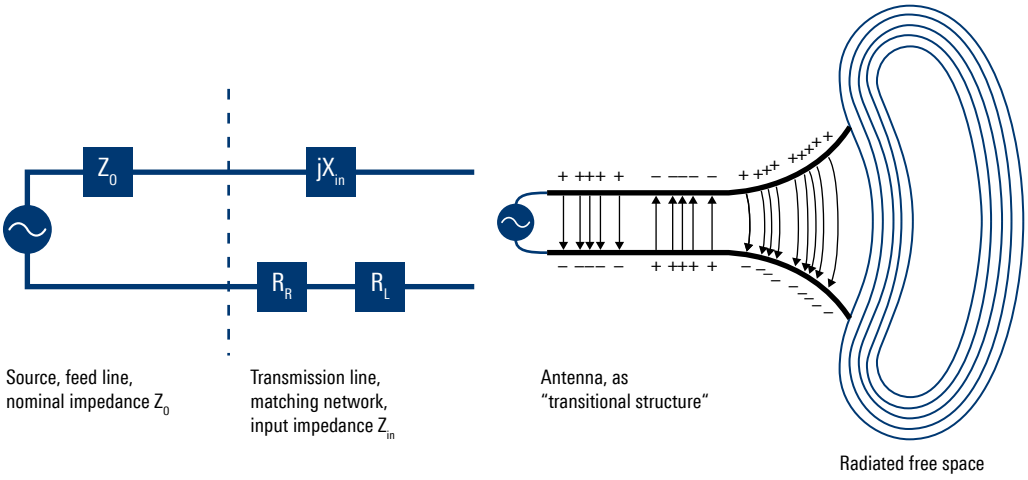

In a simplified model (see Figure 2), we may understand the antenna as a transitional structure between free space and a transmission line. The feeding network consists of the signal source and the impedance Z_0 of the generator or cable impedance, which are further connected to the antenna represented by the electric circuit. The free space or intrinsic impedance Z_L is the impedance between the perpendicular electric E and magnetic H fields and is given as 120π or 377 Ω. Since every antenna consists of real components, we model a matching network that reveals one of the key antenna parameters, i.e. its input impedance Z_{in}. This input impedance occurs at the antenna feed point or input connector. The real part consists mainly of the radiation resistance R_R and the loss resistance R_L. The imaginary part of the input impedance may be positive and inductive, or negative and capacitive. In cases where the imaginary part equals zero, the antenna is said to be at resonance.

2.1.2 Reflection coefficient and VSWR

In a real-world scenario, the antenna is connected to a generator with nominal impedance Z_0 via a length of transmission line with the same impedance Z_0 as shown in Figure 3. Because the input impedance Z_{in} differs from the nominal impedance, mismatch will occur. This mismatch is expressed by **reflection coefficient Γ**, which is defined as the ratio of the difference between antenna impedance Z_{in} and nominal impedance Z_0 and their sum.

$$\Gamma = \frac{Z_{in} - Z_0}{Z_{in} + Z_0}$$

Absolute values for gamma Γ range from –1 to +1.

Related to the reflection coefficient, two further parameters describe the quality of matching and consequently also the power transfer.

In addition to impedance, we also need to discuss antenna parameters and reflection coefficients based on power. Assuming we have a passive antenna, the signal is fed over a transmission line to the antenna. As part of a system, a certain power P_M is matched to the transmission line. Depending on the frequency-dependent matching of the antenna, some energy is reflected back, presenting a return loss, while the antenna accepts the remaining power P_{in}. The reflection coefficient Γ is the ratio of the amplitude of the reflected wave to the amplitude of the incident wave. The **return loss a_r** derives from the reflection coefficient as a logarithmic measure [Ref. 20].

$$a_r = -20 \cdot \log |\Gamma|$$

Figure 3: VSWR antenna parameter

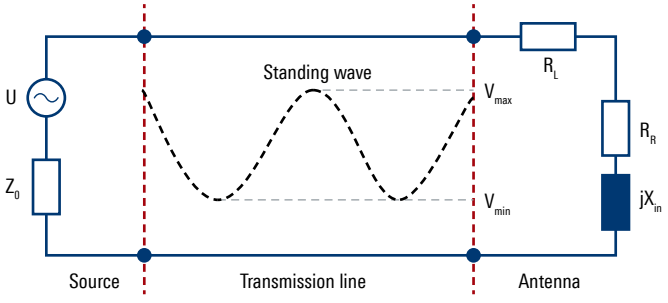

Besides reflection coefficient Γ and return loss, a third value is used in antenna measurements to indicate mismatch, the standing wave ratio. These three values can be converted back and forth and each of them describes the mismatch. Reflected waves at the interface between the transmission line and antenna create constructive and destructive interference patterns when they overlap with the waves traveling from the source. Since they resemble a standing wave in the time domain, the ratio of the standing wave is known as the **voltage standing wave ratio (VSWR)**.

$$VSWR = \frac{|V_{max}|}{|V_{min}|} = \frac{1 + |\Gamma|}{1 - |\Gamma|} > 1, \quad 1 < VSWR < \infty$$

2.1.3 Radiation power density, efficiency, intensity and isotropic radiator

Now we will look at the antenna radiating port. The radiating port is the transition from a cable or waveguide electromagnetic field to a radiated free space electromagnetic field.

Isotropic antennas are the simplest possibility. They are based on the assumption that antennas radiate power equally in all spatial directions. In our model, the radiating element is infinitely small and has spherical radiation characteristics. An isotropic radiator is used as a reference in many antenna models and also in antenna parameters such as EIRP and TIS.

Isotropic antennas are based on a theoretical model indicating that the transmitted power is spread equally over the entire surface of the sphere. It is impossible to realize an antenna which radiates equally into all spatial directions. Consequently, isotropic antennas are only used as a reference to real antenna implementations. However, we can define the **radiation power density P_{dens}** as the ratio of power P_S and the surface of the sphere. Ultimately, it is the dilution of the radiated power intensity with increasing distance from the source that provides the basis for calculating the path loss in chapter 2.1.13.

$$P_{dens} = \frac{P_s}{4\pi r^2}$$

The radiated power P_{rad} is the accepted power P_{in}, reduced by any internal losses of the antenna, e.g. resistance losses. The ratio of radiated to accepted power is the antenna **radiation efficiency η**. The **total efficiency η_t** also considers the loss caused by mismatch between the transmission line and the antenna input impedance:

$$\eta = \frac{P_{rad}}{P_{in}} \leq 1, \quad \eta_t = \frac{P_{rad}}{P_M} \leq 1, \quad \eta_t \leq \eta$$

Although we have established the ratio of power available to the antenna to the power radiated by the antenna, no particular direction of radiation has yet been discussed. The quantity used to describe the power associated with an electromagnetic wave is the instantaneous Poynting vector P = E × H [Ref. 1]. The SI unit of the Poynting vector is W/m^2, i.e. it describes a directional energy transfer per unit time and per unit area. This is known as radiated energy flux or radiated power density. Since the Poynting vector is **spatial power density**, the total power crossing a closed surface can be obtained by integrating the normal component of the Poynting vector over the entire surface S.

Relevant antenna literature, e.g. [Ref. 1] provides more details, including the mathematical background. In many applications, we encounter time-varying fields and are interested in the average power density. This is obtained by integrating the instantaneous Poynting vector over one period and using the complex fields of E and H as signal components as time harmonic variations occur [Ref. 1]. Additionally, E and H represent peak values and to obtain the RMS value, we multiply by 1/2. The power density associated with the electromagnetic fields of an antenna in the far-field region is real and known as radiation density. The radiated power based on the time-averaged Poynting vector can be written as:

$$P_{rad} = \frac{1}{2} \oiint_S Re\,(E \times H^*) \cdot ds$$

The antenna power pattern is a function of the direction of the average power density radiated by the antenna. An isotropic radiator is an ideal source, radiating equally in all directions. Integrating the complex Poynting vector over a closed sphere results in the power directed in the radial direction. Thus, it only has radial components. The total radiated power of an isotropic antenna can be written as:

$$P_{rad} = P_{dens} \cdot 4\pi r^2$$

The **radiation intensity I** in a given direction is defined as the power radiated from an antenna per unit solid angle [Ref. 1]. This parameter is valid in the far field and can be obtained by simply multiplying the radiation density by the square of the distance:

$$I = r^2 \cdot P_{dens}$$

For a closed surface, we choose a sphere of radius r and can now write the **radiated power** as the integral of radiation intensity I in all directions:

$$P_{rad} = \int_{\phi=0}^{2\pi} \int_{\theta=0}^{\pi} I(\theta, \phi) \cdot \sin\theta \, d\theta d\phi$$

Based on the IEEE antenna terminology definition, the intensity can be described in relation to the antenna feed power or the EIRP:

$$Intensity\ I = \frac{G \cdot P_0}{4\pi r^2} = \frac{EIRP}{4\pi r^2}$$

Figure 4 provides an overview of antenna parameters relevant for the following sections [Ref. 6]. Additional differences between parameters like realized gain, gain, directivity and efficiency are presented in Figure 1 and [Ref. 20].

Figure 4: Passive antenna power, gain and directivity flow chart

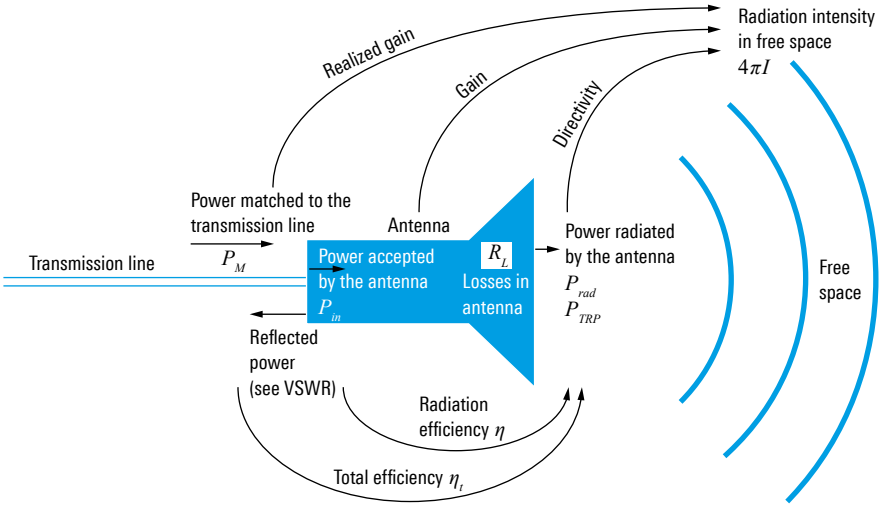

2.1.4 Passive and active antennas

Antennas are passive components that are typically considered separately. They can be combined with other components such as transceivers and amplifiers. The IEEE simply defines any antenna packaged with active devices to be an active antenna. In the

ecosystem of modern communications standards, active antennas refer to the generalized concept of having an antenna or even antenna array directly connected to the RF frontend that includes active components [Ref. 6]. Active antennas represent a way of implementing compact broadband antennas. Based on the idea of shortening the radiator, the associated change in the impedance needs to be compensated [Ref. 20].

Important in the context of this document, passive antennas are reciprocal and there is no need to distinguish between transmission and reception. Active antennas are not reciprocal. A 5G UE is considered as an active antenna device, thus reception and transmission parameters need to be analyzed separately.

With the transition to higher frequencies and advanced antenna systems (AAS) [Ref. 7], the difference between active and passive antennas has become more relevant. In a conventional antenna system, beamforming mechanisms can be supported by a single passive antenna or several passive antennas in the form of arrays combined with radio chains containing amplitude weight functions and phase shifters. Major advances in millimeterwave antennas have occurred in recent years, including integrated antennas where active and passive circuits are combined with the radiating elements in one compact unit. Active antenna systems integrate the antenna array with the transceiver frontends. Placed next to RF modules, active antennas enhance the throughput and reduce power consumption and cable losses.

2.1.5 Field regions (near field, far field) and quiet zone

The nature of electromagnetic wave propagation and radiation influences the field structure. Although there are no abrupt changes and boundaries between the field regions, significant characteristics can be observed. For better classification, the space around an antenna is subdivided into three major regions: reactive near field, radiated near field and far field. All antenna parameters are defined in the far-field (FF) region. The **antenna aperture dimension D** influences the size of these regions. In sophisticated antenna configurations, especially antenna arrays, D corresponds to the aperture size or the size of the radiating elements within the antenna system [Ref. 5].

Figure 5: Field regions

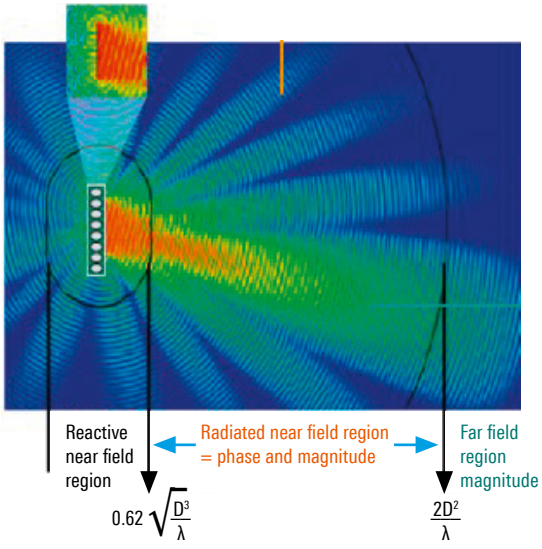

The **reactive near-field region** is the region immediately surrounding the antenna element where the reactive field predominates. For electrically large antennas, the boundary is given by the formula:

$$R < 0.62 \cdot \sqrt{\frac{D^3}{\lambda}}$$

In real-world testing, the reactive near-field region is a “no-go” zone since measurement probes or receive antennas can become radiating elements of the antenna under test due to electromagnetic coupling and results are no longer reproducible and reliable.

The **radiated near-field region** (or Fresnel region) is defined as the region where radiation fields predominate and the angular field distribution is dependent on the distance from the antenna. Measurement results depend on the amplitude and phase. As a counter-measure, it is possible to measure multiple values on a known trajectory or surface and apply postprocessing to convert the data to the far field. This is known as a near-field to far-field transformation.

The **far-field region (FF)** (or Fraunhofer region): IEEE defines the far-field to be the region where the antenna field is essentially independent of the distance from a point in the antenna region. Specifically, the angular field distribution is independent of the distance from the antenna [Ref. 3]. Plane waves can be assumed in free space and far-field distance. The Fraunhofer distance represents the boundary between the near field and far field. It is calculated for electrically large antennas as $2 \cdot D^2/\lambda$, where D is the aperture size of the antenna array and λ is the wavelength. In the far field, the electric field E and magnetic field H are perpendicular to one other and also to the direction of propagation. Moreover, there is a relationship between the two, i.e. the impedance of free space Z_L which equals 120π or about 377 Ω.

Finally, the phase of E and H is equal, meaning we can calculate H in the far field if we know E by measurements.

Quiet zone

Figure 6 illustrates the dependency of the field radiation in phase and magnitude. The objective is planar wave propagation. Assuming an infinitely small point source radiating as an ideal isotropic radiator, a phase deviation ΔΦ occurs at the edges of a surface D depending on the distance from the source and the surface size D. The concept of a quiet zone is based on the notion of accepting a measurement uncertainty below a certain threshold. At the Fraunhofer boundary, the amplitude difference is negligible over the surface D with a phase deviation ΔΦ of up to 22.5°. In other words, we obtain the size of the quiet zone corresponding to the maximum size of D, by defining a maximum threshold for the phase deviation ΔΦ that should not be exceeded.

Figure 6: Wavefront geometry

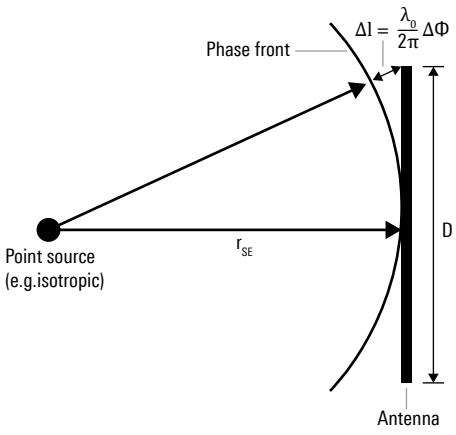

To achieve free space characteristics, the line of sight (LOS) including the first Fresnel ellipsoid between the antenna under test (AUT) and the probe antenna must be free of obstacles. Another important free space characteristic is the absence of reflections. Ideally, antenna measurements should be conducted in infinitely large rooms, which is not possible in reality. There are certain methods to emulate reflection-free environments, such as using full anechoic chambers with absorbing material at the chamber walls.

2.1.6 Directivity

Most antenna parameters are based on an ideal isotropic radiator with a constant radiation intensity in all directions. Unfortunately, such an ideal isotropic radiator does not exist in the real world. Consequently, every real antenna exhibits radiation directivity. Let us consider a simple antenna such as the half-wave dipole based on the famous Hertzian dipole model. If we measure the power density in a certain direction, we see that the resulting radiation pattern differs from the pattern for an ideal isotropic radiator. Figure 7 shows the 2D and 3D radiation pattern measurement result of a biconical antenna that is used as a real example of the theoretical Hertzian dipole antenna model.

Figure 7: Radiation patterns for a dipole antenna

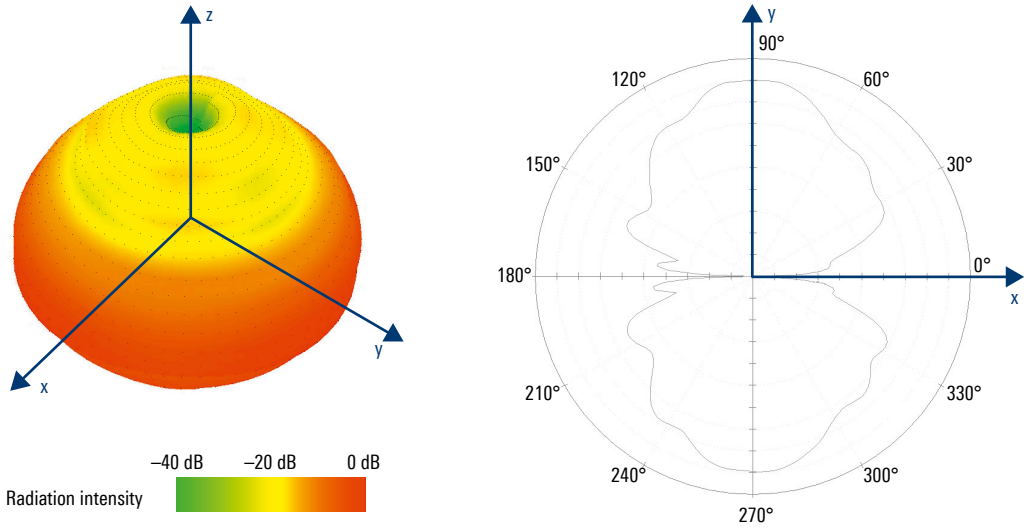

The **antenna directivity D** is the ratio of the radiation intensity in a given direction to the radiation intensity that would be produced by an isotropic radiator with the same power P_{rad}.

$$D(\theta,\phi) = \frac{4\pi\, I(\theta,\phi)}{P_{rad}} \quad or \quad \frac{I(\theta,\phi)}{I_{isotropic}}$$

Further distinction can be made by interpreting the directivity as an angular depending magnitude or as peak directivity in the main radiation direction. The directivity does not take any losses into account and only describes the relative variation of the power distribution in different directions. If the antenna has higher radiation intensity in one direction, other directions will exhibit lower radiation intensity than the spatial average. The directivity is usually expressed in decibels relative to an isotropic radiator with directivity of 1:

$$D_{dBi} = 10 \cdot \log_{10}(D)$$

2.1.7 Antenna gain

The antenna gain is the ratio of the radiation intensity in a given direction to the radiation intensity that would be produced by a lossless, isotropic radiator with the same power P_{in}. Although the gain of an antenna is closely related to its directivity, the gain considers efficiency as well as directivity.

$$G(\theta,\phi) = \frac{4\pi \cdot I(\theta,\phi)}{P_{in}}$$

The difference between gain and directivity is that the **antenna gain G** takes efficiency into account. The relationship between the two values is:

$$G = \eta \cdot D$$

In some cases, we deal with relative gain, i.e. the ratio of the power gain in a given direction to the power gain of a reference antenna in a referenced direction. Unless stated otherwise, the antenna peak gain is usually in the direction of highest directivity.

Instead of the radiation efficiency η (or the accepted power P_{in}), the total efficiency (or the available power P_M) can be used to determine the gain. This is the system-dependent **realized gain G_R** of an antenna (see also Figure 4):

$$G_R(\theta,\phi) = \frac{4\pi \cdot I(\theta,\phi)}{P_M}$$

As the gain is given in decibels, we must convert the values using logarithms:

$$G_{dBi} = 10 \cdot \log_{10}(G)$$

2.1.8 Polarization

Polarization is defined by the direction of the E field vector of an electromagnetic wave. A transmit antenna creates an electromagnetic wave with a certain orientation of the E field vector, depending on the antenna design.

Consequently, if we want to receive this signal without any loss, the receiver antenna must match that polarization – also called co-polarization.

We distinguish polarization into linear types, where the E field vector just changes its magnitude and remains in a fixed plane and circular where the magnitude of the E field vector is constant, but it constantly changes its direction. In reality, very often a mixture

of both (also called elliptical polarization) can be observed. Here the E field is changing in magnitude and direction.

Generally, any arbitrary polarization can be constructed from two orthogonal linear polarized waves with a certain amplitude and phase offset as shown in Figure 8.

Figure 8: Polarized waves and orthogonal polarization components

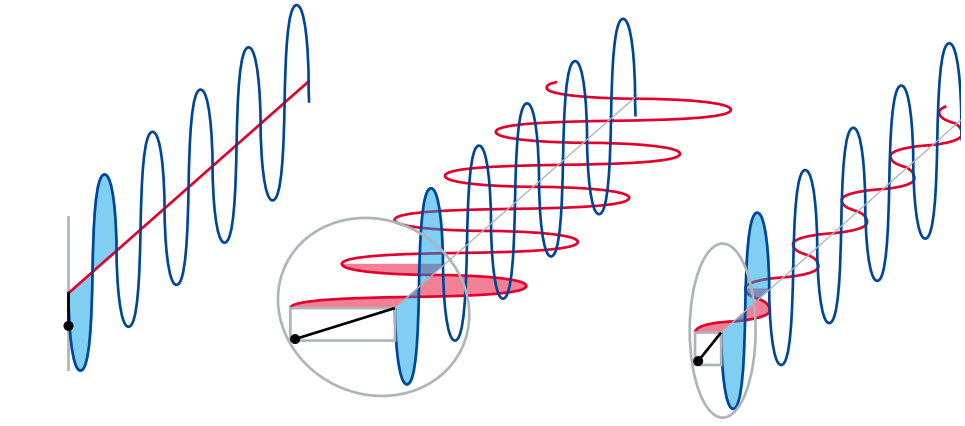

If the antenna is not co-polarized with the waves to be received, polarization mismatch will reduce the received power. In order to receive full power for arbitrary or unknown polarizations, dual-polarized probe antennas with two orthogonal polarizations can be used, particularly when measuring mobile device antennas.

2.1.9 Radiation patterns

Antenna **radiation patterns** are defined as a mathematical function or graphical representation of the radiation properties of an antenna as a function of spatial coordinates [Ref. 1]. Radiation patterns represent the spatial distribution of quantities characterizing the electromagnetic field generated by an antenna. Typical quantities are e.g. power flux density, radiation intensity, field strength, EIRP and directivity. For reciprocal antennas, the transmit and receive patterns are identical. Antenna patterns are expressed as 3D plots, 2D pattern cuts or mathematical functions. Radiation patterns allow immediate identification of the peak beam direction or unwanted side lobes. Directivity, gain or EIRP are often used for radiation pattern representation.

Figure 9: 2D and 3D radiation patterns

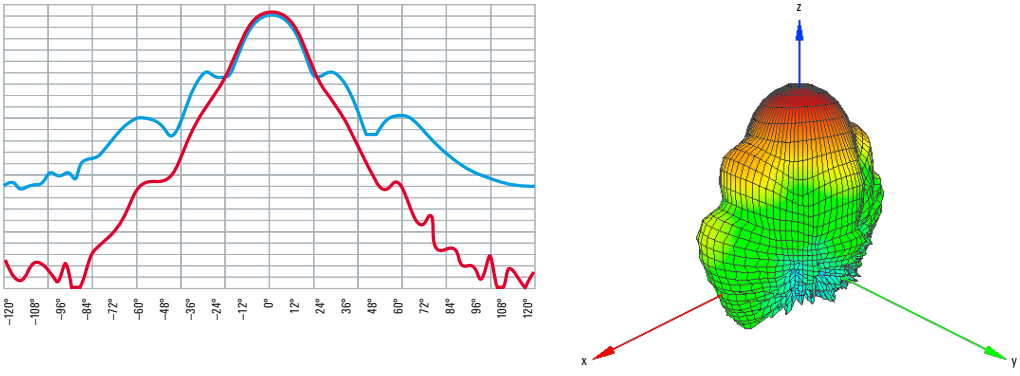

2.1.10 Equivalent isotropic radiated power

Many of the described antenna parameters such as directivity, gain, realized gain and intensity represent relative values or power ratios. The **effective or equivalent isotropic radiated power (EIRP)** denotes the absolute output power in a given direction. EIRP is the power an ideal isotropic radiator requires as input power to achieve the same power density in the given direction. This is calculated as the power accepted by the antenna multiplied by the antenna gain, or the radiated power multiplied by the directivity [Ref. 8].

$$EIRP = P_{in} \cdot G$$

$$EIRP(\theta, \phi) = P_{in} \cdot G(\theta, \phi) = 4\pi I(\theta, \phi)$$

$$EIRP_{dBm} = P_{in,\,dBm} + G_{dB}$$

EIRP is treated and measured as absolute power in watts, dBm or dBW. EIRP should be considered as a system parameter and not an antenna parameter. Given a highly directional antenna, EIRP is the power that needs to be fed to an isotropic radiator in order to produce defined radiation in a single direction that corresponds to the beam peak of this directional antenna. The beam peak is defined as the direction where maximum EIRP is detected. This statement applies to fixed antenna patterns with a static beam or to adaptive antenna patterns for which the beam can be steered accordingly.

2.1.11 Total radiated power

Total radiated power (TRP) is an active system measurement used to determine how much power is emitted or radiated when an antenna is connected to a transmitter. For lossless antennas, TRP would be equal to the input power P_{in}. It is defined as the radiation intensity at each angle in watts per steradian (Θ, Φ) integrated over the whole sphere around the antenna. Thus, we need to compute the integral across a virtual full sphere around the origin (antenna position) at far-field distance r. Note that in the far field, the Poynting vector is orthogonal to the sphere surface, i.e. it has a radial component only. The magnitude of this radial component corresponds to the power density ρ at this point. Since the power density is defined as the actual EIRP value divided by the spherical surface area ($4\pi r^2$), the virtual radius r is irrelevant in the TRP calculation as long as it is constant.

The power radiated by the antenna (P_{rad}) is also known as the total radiated power (P_{TRP}). It is defined as the radiation intensity (Θ, Φ) integrated over the whole sphere around the antenna.

$$P_{TRP} = \frac{1}{4\pi} \int_{\phi=0}^{2\pi} \int_{\theta=0}^{\pi} EIRP(\theta, \phi) \cdot \sin\theta \, d\theta d\phi$$

Ideally, we need to measure the EIRP at every elevation and azimuth angle and integrate the power over the entire sphere surrounding the antenna [Ref. 9].

Figure 10: TRP integral

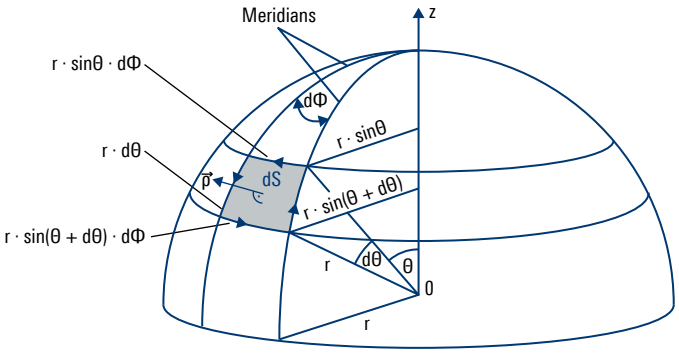

In the far field, the radiation intensity can be defined as:

$$I(\theta,\phi) = \frac{EIRP(\theta,\phi)}{4\pi}$$

Using this definition of the radiation intensity, it is possible to rewrite the TRP integral:

$$P_{TRP} = \frac{1}{4\pi}\int_{\phi=0}^{2\pi}\int_{\theta=0}^{\pi} EIRP(\theta,\phi)\cdot\sin\theta\, d\theta d\phi$$

Since we typically perform measurements in discrete steps, the integration is transformed into a sum over all measured EIRP values.

$$TRP \approx \frac{\pi}{2NM}\sum_{i=1}^{N-1}\sum_{j=0}^{M-1}\left(EIRP_{\theta}(\theta_i,\phi_j) + EIRP_{\phi}(\theta_i,\phi_j)\right)\sin(\theta_i)$$

The measurement is performed by placing the DUT in an anechoic chamber on a two-axis positioning system. The DUT is positioned at different coordinates in a spherical coordinate system. The transmitted power is sampled at equally spaced increments of Φ and Θ over the entire sphere surrounding the DUT. These relative power measurements are converted to effective isotropic radiated power (EIRP) using a range reference measurement. Finally, the EIRP values are weighted by sin(Θ) and summed to calculate the total radiated power. The sin(Θ) weighting compensates the increasing density of samples towards the poles.

2.1.12 Equivalent isotropic sensitivity and total isotropic sensitivity

Besides the TX direction, system parameters can also characterize the RX performance. Antenna performance is measured by monitoring quantities such as BER, BLER, FER or data throughput when the RX power level decreases. The sensitivity indicates when this quantity drops below a threshold value. EIS is the **effective or equivalent isotropic sensitivity (EIS)** of the receiver in a given direction. It is determined iteratively by decreasing the transmit power of the test signal and monitoring the sensitivity quantity, e.g. BER. If the DUT is a directional antenna, e.g. an AAS array, the effective isotropic sensitivity (EIS) is defined as the power level relative to an isotropic antenna that is incident on the AAS array from a specified azimuth/elevation direction (angle of arrival) in order to meet the specified receiver sensitivity requirement. Here, the angle of arrival can be described as a combination of Φ and Θ, i.e. as the azimuth and elevation in a spherical view [Ref. 6].

The **total isotropic sensitivity (TIS)** is a measure of the overall RX quality of a system under test. For each point on the sphere (azimuth, elevation and polarization) with a given step size in the angular grid, a reference signal arrives from the corresponding direction.

The received signal quality (e.g. BER, BLER or throughput) is measured as a function of RX power level and sensitivity (EIS).

$$TIS = \frac{4\pi}{\int_0^{2\pi}\int_0^{\pi}\left(\frac{1}{EIS_\theta(\theta,\phi)} + \frac{1}{EIS_\phi(\theta,\phi)}\right) sin\theta \; d\theta \; d\phi}$$

In real-world measurement systems, the test is performed in discrete steps. Thus, the integral becomes a summation:

$$TIS \approx \frac{2NM}{\pi \sum_{i=1}^{N-1}\sum_{j=0}^{M-1}\left(\frac{1}{EIS_\theta(\theta_i,\phi_j)} + \frac{1}{EIS_\phi(\theta_i,\phi_j)}\right)\sin(\theta_i)}$$

2.1.13 OTA losses: free space path loss (FSPL)

The transmission equation postulated by Harald Friis relates the power received by an RX antenna to the power transmitted by a TX antenna separated by a distance greater than the Fraunhofer distance [Ref. 10]. The power relationship is given as:

$$\frac{P_{RX}}{P_{TX}} = G_{antenna} \cdot \left(\frac{c}{4\pi f d}\right)^{\gamma}$$

The antenna gain given here is a combination of RX and TX antenna gain. The exponent γ represents the loss of the medium between both antennas, e.g. foliage, building material, rainfall or just open airspace. Assuming the OTA tests are performed in a full anechoic chamber where only air (with γ = 2) lies between TX and RX, the equation becomes the following:

$$P_{RX} = P_{TX} G_{TX} G_{RX} \left(\frac{\lambda}{4\pi d}\right)^2$$

Rearranging, we obtain:

$$P_{RX} = P_{TX} G_{TX} G_{RX} \left(\frac{\lambda^2}{4\pi}\right)\left(\frac{1}{4\pi d^2}\right)$$

We can imagine the term $1/(4\pi d^2)$ as corresponding to the surface of a sphere. Therefore, our notion of free space path loss does not involve any real loss. Instead, it is the spherical dilution of the radiated power intensity at increasing distance from the source.

The loss of signal power over the air predominates in typical OTA test systems. For the sake of simplicity, we use power ratios to transform the equation into a summation where the quantities are in decibels. The **free space path loss (FSPL)** is defined as follows [Ref. 6]:

$$FSPL\ (in\ dB) = 20 \cdot \log_{10}(d) + 20 \cdot \log_{10}(f) - 147.55$$

d is the distance between the antennas in meters, f is the frequency in Hz, and $d \gg c/f$ must hold.

The calculation of FSPL assumes isotropic radiators as the transmit and receive antennas. Since the antenna gain is also relative to an isotropic radiator, the actual OTA loss can be easily calculated using FSPL and the antenna gain in dB and dBi, respectively.

Besides OTA loss, cable losses must also be considered. Since they are defined in decibels per unit length, the loss in dB increases linearly with distance. However, the FSPL in dB increases logarithmically with distance. While FSPL increases slowly at greater distances, it is much higher at typical measurement distances compared to cable losses. Nevertheless, cables contribute considerable losses to the overall system, especially in the millimeterwave bands. A 1.5 m test range at 30 GHz has an FSPL of 65.5 dB. 10 m of cables with a loss of 3 dB/m add an additional 30 dB. T&M equipment must have a large dynamic range to handle the combined losses in mmWave OTA systems.

2.1.14 Beamforming

Sophisticated antennas provide high directivity. With the multi-user MIMO approach, beamforming increases the RX power level, mitigates interference to other users and enhances overall system efficiency. For further information, see the relevant beamforming literature [Ref. 4].

Beamforming antennas use antenna arrays to achieve directional signal transmission and reception. To change the direction of the array, a beamformer adjusts the phase and amplitude of the signal at each antenna element. The direction Θ of the beam depends on the antenna spacing d, wavelength λ and phase shifts between the antenna elements. Note that the beam steering capability of an antenna array is only valid for a certain angular range. Distancing from the boresight direction, the radiated power on a certain beam will decline and the half-power beamwidth widens up. This effect is described as scanning loss. A countermeasure, performed in several commercial handsets, is to equip the device with multiple antenna arrays to cover the best beam coverage.

Analog, digital and hybrid beamforming schemes are known. Hybrid beamforming is most commonly used in 5G FR2. Note that phase shifts alone would be sufficient to achieve beam steering in different directions. However, the ability to change the amplitude enables optimization of the side lobe suppression [Ref. 7].

Figure 11: Beamforming and beamsteering principle

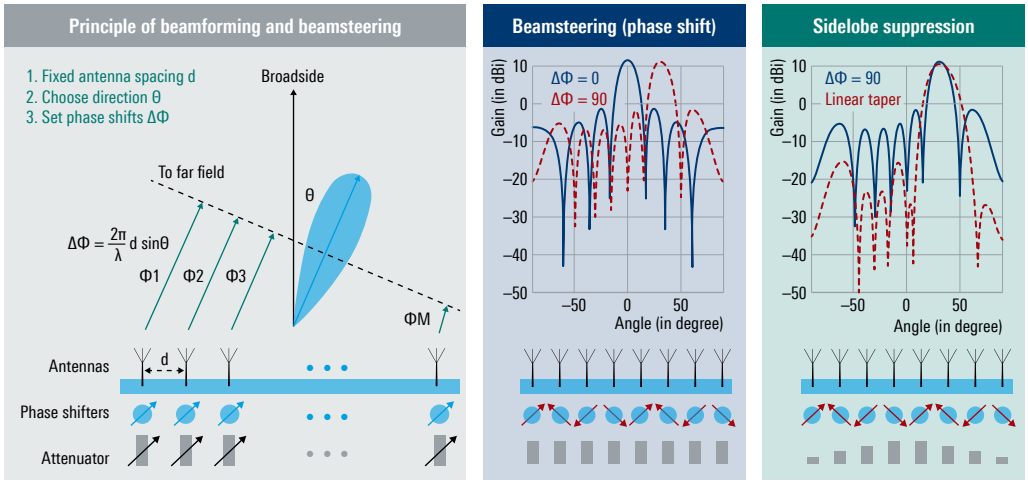

The introduction of antenna beamforming makes OTA measurements mandatory because there is no other way to connect the AUT to the measurement antenna. Since beamforming requires analysis of the radiation behavior in the spatial domain, there are some new antenna parameters:

Beamwidth: This parameter describes how narrow the beam is. It is defined as the half-power beamwidth (HPBW), i.e. the width of the beam based on the half power of the beam peak.

Beam peak: 3D direction or elevation and azimuth angle of highest directivity. Figure 12 shows a real measurement result.

Beam center: 3D direction or elevation and azimuth angle for the center angle of the 3 dB beam. Note that the beam peak and beam center may deviate.

Beam peak direction: The 3GPP defines the TX beam peak direction as the direction where the maximum EIRP is detected and the RX beam peak direction as the direction where the maximum sensitivity EIS is detected.

Figure 12: Half-power beamwidth, beam peak and beam center

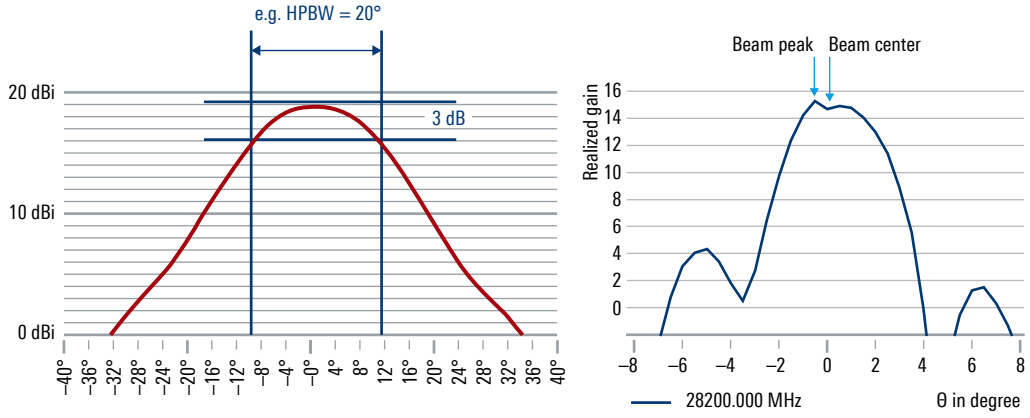

3 OTA SYSTEMS

3.1 Methods for radiated RF field testing

Currently, there are three accepted RF conformance testing methods, all of which ensure far-field conditions for testing (TR37.941):

- Direct far field (DFF)
- Indirect far field (IFF), also known as CATR
- Near-field to far-field transformation (NF-FF)

Figure 13: Direct far-field (DFF) OTA test setup

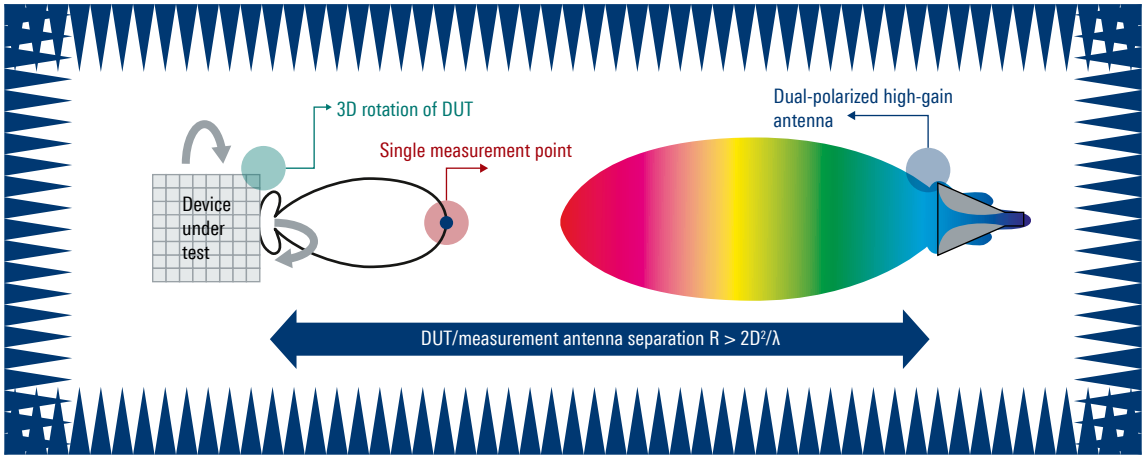

Figure 14: Indirect far-field (IFF) OTA test setup

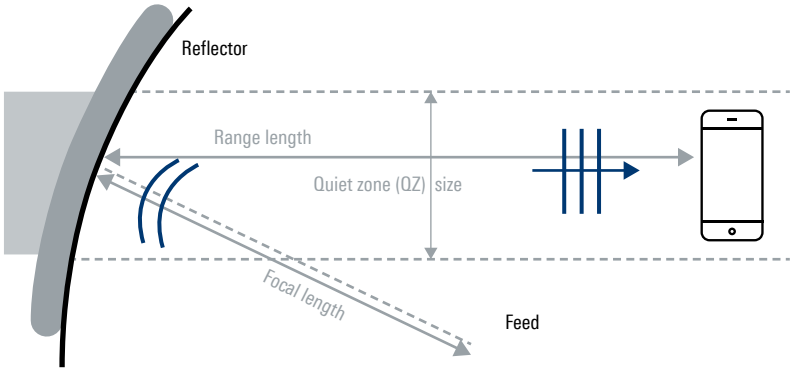

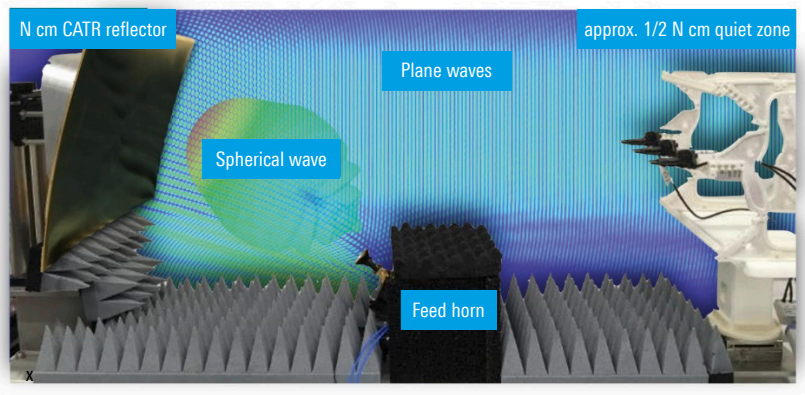

Figure 15: Near-field (OTA) test setup with computational NF-FF postprocessing

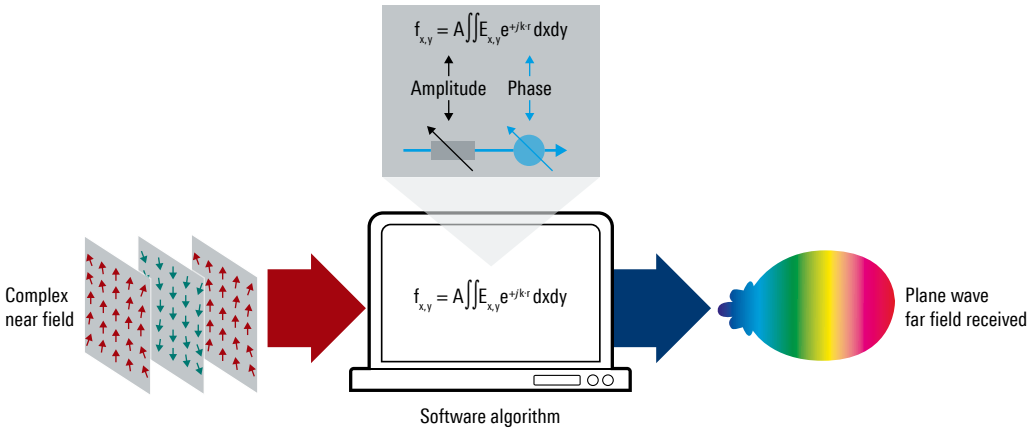

In a typical test setup, these three methods are applied by placing the DUT and measurement antenna in a full anechoic chamber (FAC) in order to provide shielding and suppress reflected DUT emissions. The advantage of the NF-FF postprocessing method is the smaller FAC size requirement. However, due to time dependencies and the need to measure over a geometrical surface [Ref. 12], this method is cumbersome for metrics such as EVM or ACLR and receiver sensitivity. Assuming the DUT is a UE, the relevance of each of the three methods is determined primarily by quantity, size and position of the arrays within the DUT. DFF and IFF are possible test methods for UEs with either a single antenna array or multi-antenna array. However, only one array may be active at any time and the array under test must be positioned in the relevant quiet zone. For UEs with large antenna arrays, typically the quiet zone achieved with DFF is too small. Due to the near-field characteristics and higher measurement uncertainty, this test method is not suitable for high accuracy EVM and RX sensitivity measurements.

The size of the quiet zone (QZ) limits the maximum size of the DUT. The requirements for the QZ size depend on the specific implementation. Knowledge of the antenna aperture is necessary. Here, black box and white box testing are relevant. Given a DUT with typical smartphone dimensions but no information about the exact position of the antenna array within the DUT, the black box approach is required. In other words, we must assume the worst case for the aperture size, i.e. the DUT size. In white box testing, the antenna array size and position are known beforehand. Figure 16 illustrates the required distance to obtain the relevant quiet zone. Assuming a DUT size of 12 cm and a 5G NR FR2 carrier frequency of 39 GHz, far-field conditions are obtained for a distance of approximately 390 cm (approx. 4 m) between the DUT and measurement antenna. However, if we know that the antenna array has a size of approx. 3 cm along with its exact position within the UE, the distance shrinks to approx. 30 cm. Obviously, white box versus black box testing has a major impact on the full anechoic chamber size [Ref. 11].

Figure 16: Black box and white box testing versus quiet zone size requirements/frequency

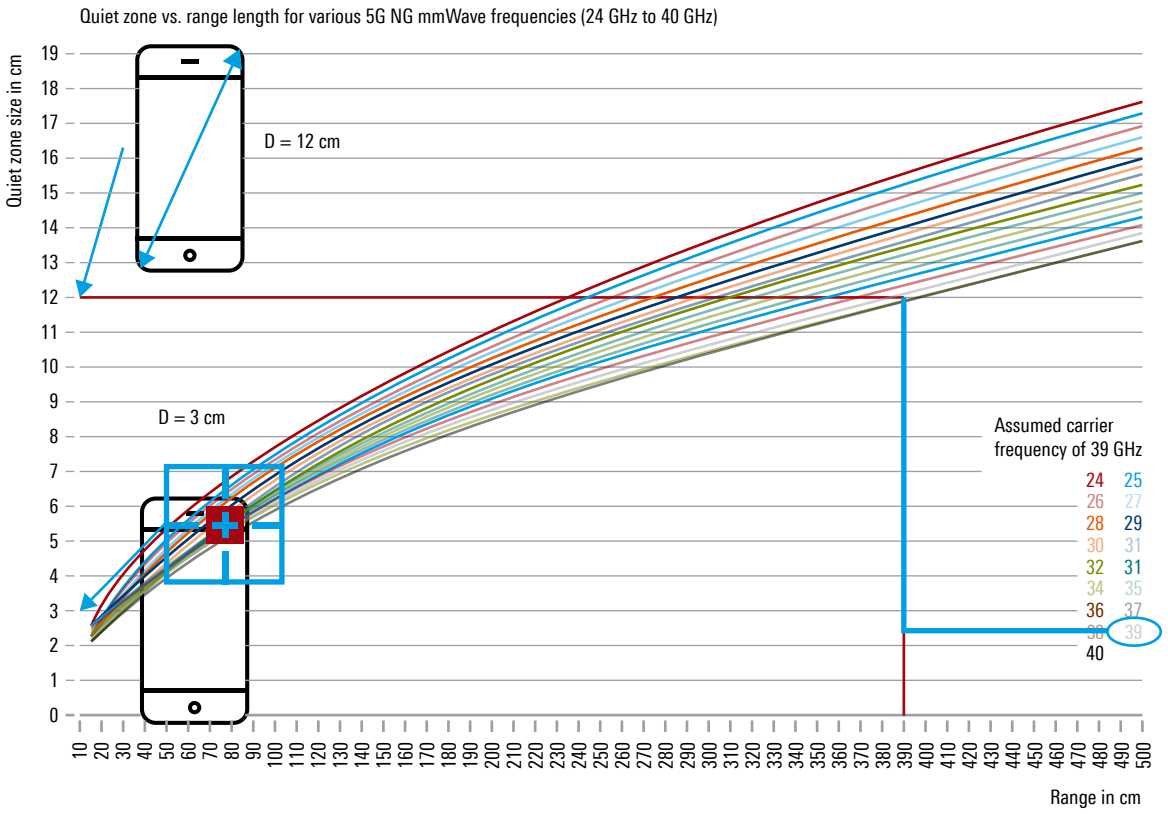

3.2 Near-field measurements and NF-FF transformation

Since the Fraunhofer distance that applies to far-field conditions depends on the aperture size and frequency, the dimensions of the required test setup, especially the size of a full anechoic chamber, can be huge. The test setup can become impractical due to complexity, cost and size. An alternative is to perform antenna measurements in the near field and use computational methods to transform the measured near-field data into far-field characteristics. Such methods are described in the relevant literature, e.g. [Ref. 1], [Ref. 12] and [Ref. 13].

Measurements in the near-field region require both the field phase and magnitude sampled over an enclosed surface (spherical, linear or cylindrical) in order to calculate the field magnitude using Fourier spectral transforms.

This measurement is typically performed using a vector network analyzer with one port connected to the DUT. Furthermore, we need both orthogonal polarization planes, so that two ports are connected to the dual polarized measurement antenna. For active antennas or massive MIMO configurations, however, dedicated antenna or RF ports are usually unavailable. OTA measurement systems must therefore be able to retrieve the phase in order to complete the transformation into the far field. Two methods are common in the industry [Ref. 5]. The first method is an interferometric technique using a second antenna with a known phase as reference. This phase reference antenna must be fixed with respect to the DUT. The signal is mixed with the DUT signal with unknown phase. The main idea is that the phase of interest is the electromagnetic propagation phase (as opposed to the phase shift due to modulation). To eliminate modulation-related phase variations, a measurement device with two synchronous acquisition ports can be used. This device acquires signals from the measurement antenna and the reference antenna. It extracts only the propagation-related phase of interest using postprocessing algorithms.

The second method uses multiple surfaces or probes as phase reference. A constant distance of either a half or full wavelength is required between the surfaces or probes. Disadvantages of this method are the increased measurement time and test setup complexity (especially the calibration).

3.3 Grid types, quiet zone aspects, coordinate system

Many antenna parameters are defined with respect to a spherical surface that serves as a "measurement" surface. For radiated test setups, a reference coordinate system is required to provide a clear and traceable link between the measurement samples at a given spatial position and the DUT position. The goal is to convert the system from the traditional Cartesian to the polar coordinate system. The Cartesian coordinate system is a reference system with perpendicular axes x, y, z and spherical angles Θ, Φ. IEEE standard 149-1979 "IEEE Standard Test Procedures for Antennas" [Ref. 2] defines a reference coordinate system based on the azimuth angle Φ and elevation angle Θ.

Figure 17: Reference coordinate system

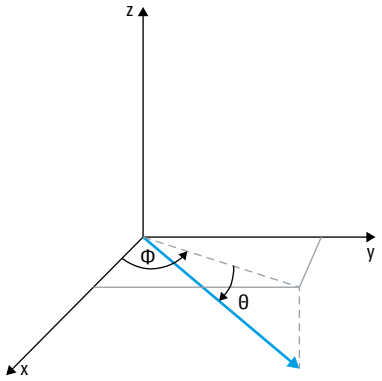

Because certain measurements must be made at a defined spatial position and certain values require computation of a sum or integration, the TR 37.941 standard for base station OTA testing defines multiple grids. 2D or 3D cuts are applied depending on the desired radiation pattern. An equal angle grid uses constant angular steps to acquire the radiated measurement samples. This allows easier handling with mechanical positioning systems, but produces a variable density for the samples over the spherical surface. The advantage of positioning systems with distributed rotation axis is that one axis moves continuously while the other axis is stepped, resulting in faster measurement speed. The problem of the fluctuating sample density can be solved using an equal area grid approach where the spherical distance between two neighbor samples is constant [Ref. 8]. The challenge of this grid approach is the non-constant step size, necessitating higher accuracy in the positioning system. In a distributed axis positioning system, both axes are required to move. The optimum path between the measurement points must be determined to reduce the overall test time.

Figure 18: 2D-cut grid and 3D-cut grid

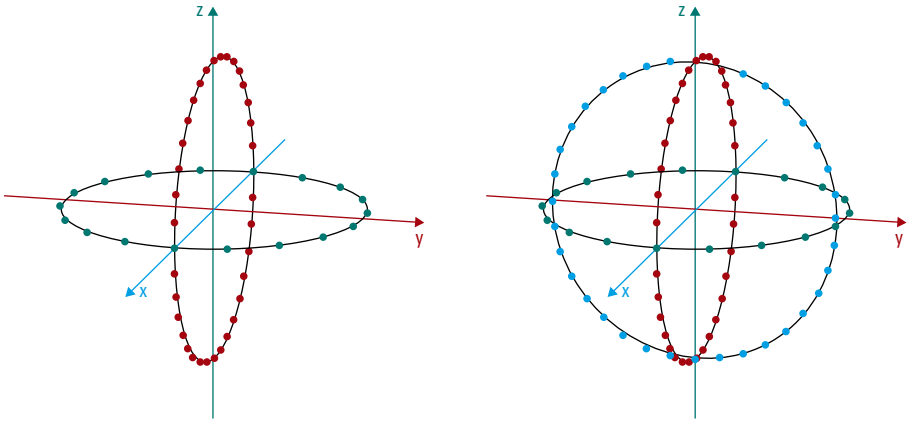

Figure 19: Equal angle grid and equal area grid

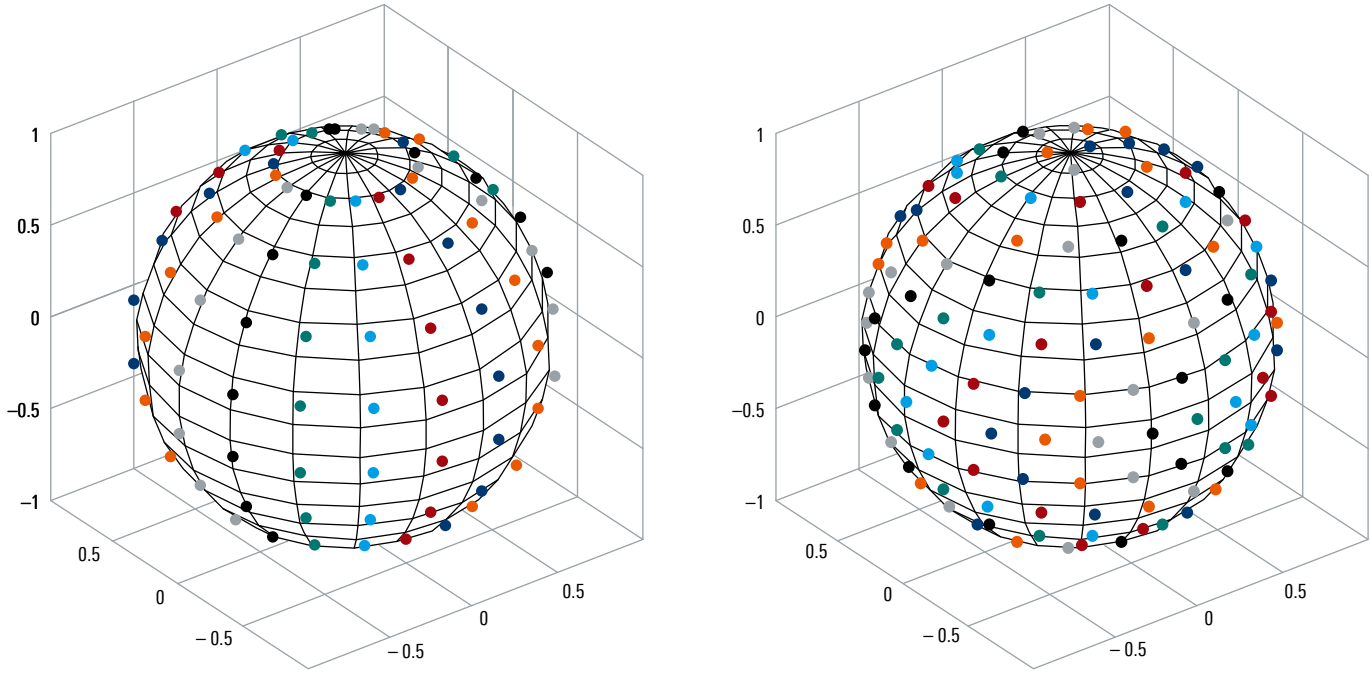

In real-world OTA setups, there are two major positioning systems that allow a spherical scan: **conical cut** or **azimuth over elevation cut** [Ref. 19]. The difference is related to whether the two rotation axes are combined within the setup or distributed.

Figure 20: Spherical scan systems: conical cut versus azimuth over elevation cut

Conical cut = distributed axis
e.g. R&S®ATS1000 or R&S®WPTC

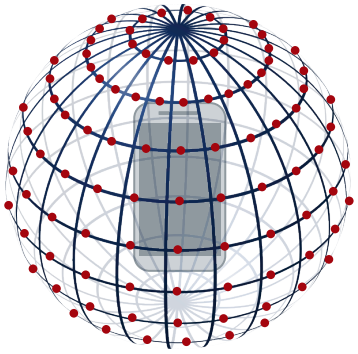

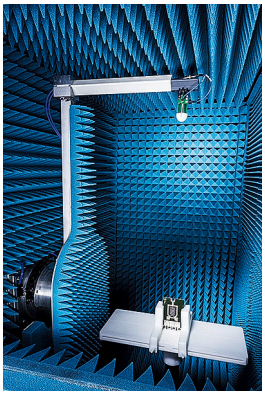

Azimuth over elevation cut = combined axis
e.g. R&S®ATS1800C

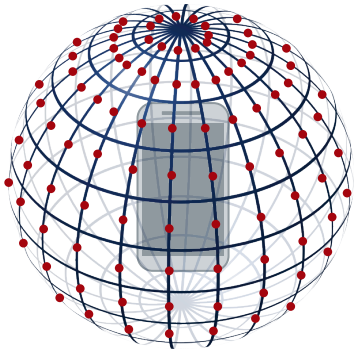

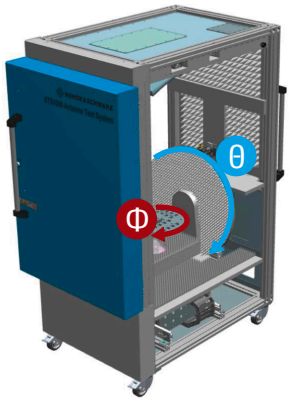

3.4 Direct far field, e.g. R&S®ATS1000

For RF testing, there are two main approaches: the direct far-field (DFF) and the indirect far-field (IFF) method (TS 38.521). Both use an anechoic chamber for shielding. A positioning system is required such that the angle between the dual-polarized measurement antenna and the DUT has at least two axes of freedom and maintains a polarization reference. The DFF method allows measurements at a sufficiently large distance according to the Fraunhofer distance [Ref. 17]. The chamber must fulfill two major requirements: shielding against emissions from outside the chamber and mitigation of reflections within the chamber. A **full anechoic chamber (FAC)** simulates an infinitely large room without any reflections or interfering signals. Absorbent material on the chamber surfaces prevents reflected signals. Note that the absorber reflectivity depends on the cone shape, the angle of incidence and size of the absorbers [Ref. 14]. Shielding such as metallic layers within the walls attenuates external signals.

The R&S®ATS1000 antenna test system [Ref. 15] is a shielded chamber solution for various antenna testing applications. It fulfills all of the test requirements for 3D antenna pattern characterization and antenna system characterization. The system performs fast and reliable measurements under direct far-field conditions in a fully anechoic chamber over a wide frequency range from 18 GHz to 50 GHz. Moreover, the high-precision conical cut positioner allows movements with extremely high repeatability and an angular resolution of 0.03° for both azimuth and elevation. Since the radiation patterns of miniaturized antennas can be influenced by temperature, thermal diagnosis is gaining traction. The R&S®ATS1000 can be retrofitted with a temperature testing option to perform fast and precise 3D thermal measurements from –40 °C to +85 °C [Ref. 15].

Figure 21: R&S®ATS1000 direct far-field test setup including temperature test solution

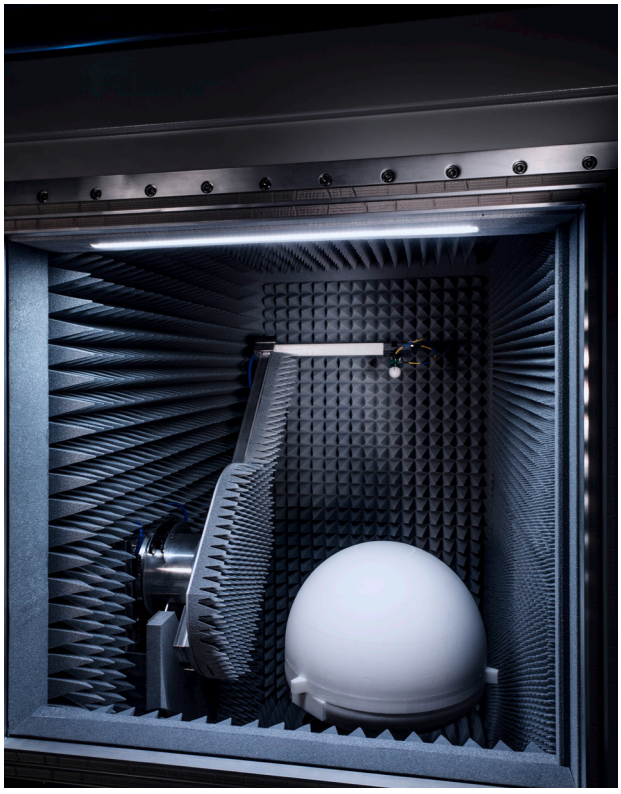

3.5 CATR principles

The IFF method uses a hardware transformation of the propagating waves to create plane waves, i.e. far-field conditions, at the DUT at a distance less than the Fraunhofer distance. The parabolic shape of the reflector transforms spherical waves to plane waves when the probe antenna is placed in the reflector's focal point. This reduces the required chamber size along with the cost of the test setup. Additionally, the IFF method allows better control and parametrization.

This solution is also known as **compact antenna test range (CATR),** as illustrated in Figure 22. According to Fermat's principle of least time, a planar wave can be focused on a single point using a parabolic mirror. If a measurement antenna is placed at this focal point, using the reciprocity principle, a planar wave can be generated since the parabolic mirror reflects a certain planar component of the incoming spherical wave from the measurement (or feed) antenna into the quiet zone where the DUT is placed.

Figure 22: Compact antenna test range (CATR)

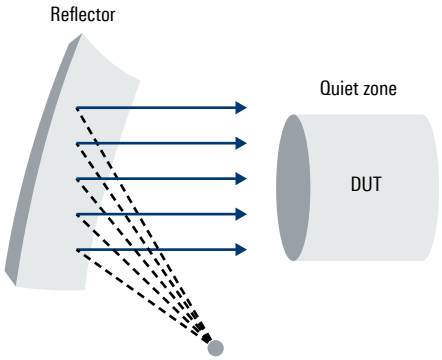

Major compact range drawbacks include aperture blockage, direct radiation from the source to the test antenna, diffraction from the edges of the reflector and feed support, depolarization coupling between the two antennas, and wall reflections [Ref. 1]. The quality of the quiet zone is diminished by an amplitude taper caused by the feed antenna pattern, amplitude ripples due to imperfections and residual scattering, as well as phase taper and ripple [Ref. 6].

Key CATR reflector design parameters include the reflector size and material, edge treatment and surface roughness. The reflector edge shape determines the quality and size of the quiet zone. The surface roughness affects the power tapers of the quiet zone. Both design parameters (roughness and edge treatment) determine the frequency range of the parabolic reflector. The surface roughness causing power ripples sets the upper frequency boundary and the edge scattering defines the lower frequency. As rules of thumb, the size of the antenna aperture under test should be about 25 % to 50 % of the size of the CATR reflector, and the surface roughness of the reflector should be under λ/100 [Ref. 16].

Figure 23: CATR design parameters for edge treatment

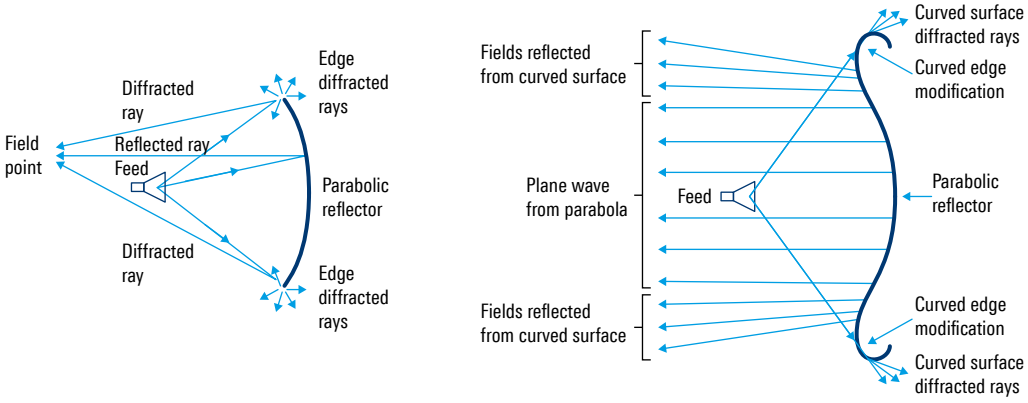

Figure 24: CATR design parameters for surface roughness

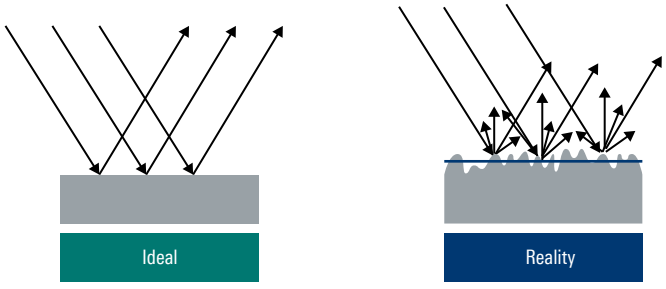

3.6 Plane wave converter

In the 5G FR1 range under 6 GHz, large antenna aperture sizes may be assumed. One CATR drawback is the reflector size, which is around two to four times as large as the AUT. It is impossible or costly to manufacture such a large parabolic reflector while fulfilling relevant accuracy requirements. This is due to weight, surface roughness and fabrication cost issues. Plane wave synthesis provides an innovative, lightweight and cost-effective way to emulate far-field conditions. This method is also accepted by the 3GPP for testing large AUT apertures such as base stations [TR 37.941]. By combining the radiation of multiple antennas assembled in a phased antenna array and fed with predetermined signal magnitude and phase, plane wave conditions are created within a defined quiet zone. The R&S®PWC200 system consists of an array of 156 wideband Vivaldi antennas and a beamforming network of phase shifters and attenuators at the back. This R&S®PWC200 array is 1.8 m wide and creates a spherical quiet zone of 1 m diameter at a distance as short as 1.5 m in the frequency range covering parts of FR1. Since this paper focuses on UE OTA testing, we only mention the plane wave synthesis method for the sake of completeness. Details can be found in [Ref. 18].

3.7 OTA test setup calibration

In order to conduct accurate antenna parameter measurements, the system must be carefully calibrated. The first negative aspect to consider is the previously mentioned free space path loss. In other words, an OTA link has a frequency-dependent loss that is generally very high compared to conducted tests. This is true especially under far-field conditions where the distance between the measurement antenna and DUT is large. Moreover, while a cable of a certain length has fixed attenuation, the OTA measurement distance can easily and inadvertently change, causing differences in attenuation and especially phase. The DUT should be placed in the rotation center of the positioning system. Deviations occur even for small positioning errors or mechanical imperfections of the test fixture when rotating the DUT.

Various methods are available for tackling calibration issues, using different setups and instruments. A vector network analyzer can measure the S-parameters (the S_{21} value corresponds to P_{TX} and P_{RX} as described below) and helps determine the antenna gain or system loss L_{sys}, respectively. Modern signal generators and signal or spectrum analyzers allow large bandwidth and modulated signals.

Figure 25: Generic OTA setup block diagram

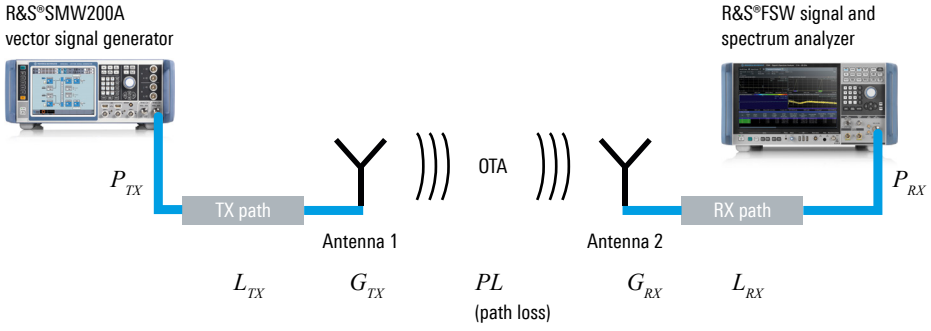

The easiest way to determine the AUT gain is to compare the unknown antenna to a known reference antenna, e.g. as shown in Figure 25, where “Antenna 1” represents the AUT. With the gain substitution technique (gain transfer method), a reference antenna with known gain G_{ref} is placed at the location where the AUT is to be placed. L_{sys} represents the overall path loss including the values L_{TX}, OTA free space path loss PL and L_{RX} in Figure 25. P_{TX} is the transmitter power for the AUT and reference antenna that is kept on the same value. $P_{RX, ref}$ and $P_{RX, AUT}$ are the power levels received with the system reference and AUT antennas, respectively. G_{ref} is the known reference antenna gain, and G_{AUT} is the

unknown AUT antenna gain. By measuring the full setup with both antennas and comparing the results, the gain of the unknown antenna can be determined:

$$L_{sys} = P_{TX,\,ref} + G_{ref} - P_{RX,\,ref}$$

$$G_{AUT} = P_{RX,\,AUT} + L_{sys} - P_{TX,\,AUT}$$

With $P_{TX} = P_{TX,\,ref} = P_{TX,\,AUT}$ and inserting the system loss L_{sys}:

$$G_{AUT} = G_{ref} + P_{RX,\,AUT} - P_{RX,\,ref}$$

Further details on OTA test setup calibration are provided in [Ref. 6] and [Ref. 8].

4 3GPP FR2 CONFORMANCE MEASUREMENTS

The 3GPP RAN5 working group is responsible for specifying conformance test cases. Test specifications are organized as follows.

Table 1: 3GPP conformance test specifications

Specification	Scope
3GPP TS 38.521-1	UE RF conformance FR1 standalone test
3GPP TS 38.521-2	UE RF conformance FR2 standalone test
3GPP TS 38.521-3	UE RF conformance FR1 and FR2 non-standalone test
3GPP TS 38.521-4	UE RF conformance performance test
3GPP TS 38.533	UE RRM conformance test

The listed test specifications refer to the following common specifications and technical reports.

Table 2: 3GPP conformance test reference documents

Specification	Scope
3GPP TS 38.508-1	UE conformance specification; part 1: common test environment
3GPP TS 38.508-2	UE conformance specification; part 2: common implementation conformance statement (ICS) proforma
3GPP TS 38.509	Special conformance testing functions for UE
3GPP TR 38.810	Study on test methods for new radio
3GPP TS 38.101-1	UE radio transmission and reception; part 1: range 1 standalone
3GPP TS 38.101-2	UE radio transmission and reception; part 2: range 2 standalone
3GPP TS 38.101-3	UE radio transmission and reception; part 3: range 1 and range 2 interworking operation with other radios
3GPP TS 38.101-4	UE radio transmission and reception; part 4: performance requirements
3GPP TS 38.133	Requirements for support of radio resource management

All listed 3GPP specifications along with all other 5G NR documents are available for free on the 3GPP portal at www.3gpp.org.

Since this document focuses on frequency range 2 (FR2), 3GPP TS 38.521-2 is the main reference. 3GPP TR 38.810 "free space" testing is the default test configuration. All UEs supporting NR and operating in FR2 must support the following conformance test specific functions:

- A **UE beam lock function** (UBF) must be provided to reduce test method complexity. This allows the UBF to disable changes to UE beamforming while testing a selected parameter
- Measurement and reporting of the **synchronization signal reference signal received power per branch** (SS-RSRPB) must be supported

Each test method must allow testing of the following RF metrics and parameters:

Transmitter metric

- Total radiated power (TRP)
- Beam peak EIRP
- Uplink spherical coverage
- Transmit signal quality including frequency accuracy, EVM and spectral flatness
- Radiated spurious emissions

Receiver metric

- Beam peak EIS
- Reference receiver sensitivity
- Downlink spherical coverage
- Adjacent channel sensitivity
- Maximum input level
- Blocking

For the UE RF test methods in FR2, the following general aspects apply:

- Over-the-air (OTA) measurement is the default test method
- Permitted OTA test methods are defined in 3GPP TR 38.810 and must demonstrate equivalence to far-field environments

All OTA test setups are located in an **anechoic chamber (AC)** in line with 3GPP and support one of the following principles:

Direct far field (DFF)

- A DFF measurement setup must be capable of **center of beam** and **off center of beam** measurements
- A positioning system must ensure that the angle between the **dual-polarized measurement antenna** and/or **link antenna** and the DUT has **at least two axes of freedom** and maintains an electromagnetic field polarization reference (Figure 26)
- In view of the far-field criterion (**$R > 2D^2/\lambda$**), the DUT radiating aperture must not exceed 5 cm (which also determines the minimum size of the quiet zone in which the radiating aperture under test is to be placed)
- A manufacturer declaration regarding the radiating aperture size and location is required ("white box testing")
- All metrics such as EIRP, TRP, EIS, EVM, spurious emissions and blocking can be tested
- **The R&S®ATS1000 antenna test system provides a 3GPP compliant DFF environment** [Ref. 15]

Figure 26: DUT positioning in a DFF setup (allows repositioning due to shadowing)

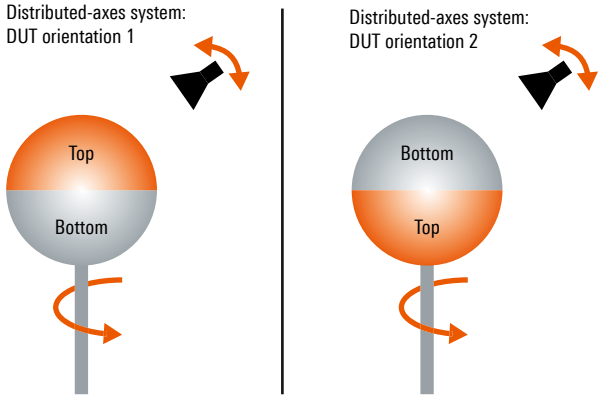

Indirect far field (IFF)

- The IFF method creates a far-field environment using an electromagnetic field transformation with a parabolic metal reflector (Figure 27). This is also known as the **compact antenna test range (CATR)**
- An IFF measurement setup is capable of **center of beam** and **off center of beam** measurements
- The total test volume is a cylinder (quiet zone) and the DUT must fit within the total test volume for the entire duration of the test
- No manufacturer declaration regarding the radiating aperture is needed
- All metrics such as EIRP, TRP, EIS, EVM, spurious emissions and blocking can be tested
- **The R&S®ATS1800C antenna test system provides a 3GPP compliant IFF environment** [Ref. 19]

Figure 27: DUT positioning in an IFF setup (allows repositioning due to shadowing)

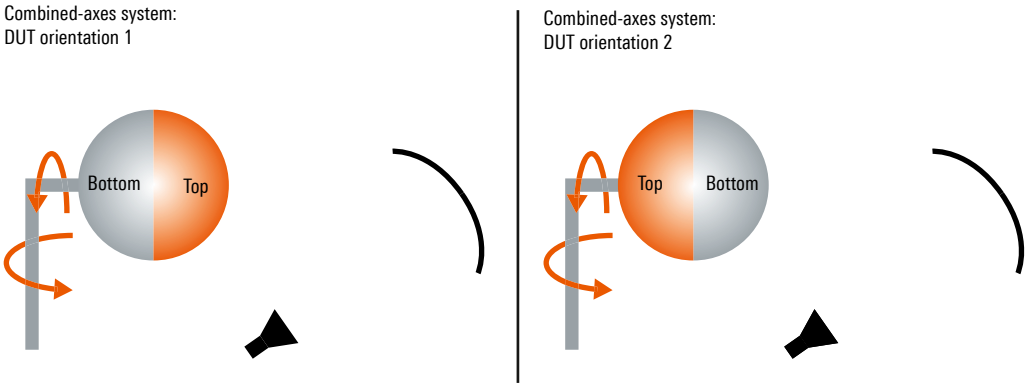

Other methods are based on near-field to far-field (NF-FF) transformation. However, such methods require phase information using a reference signal and only support transmitter measurements. Accordingly, they are not very efficient and of minor importance.

The following chapters contain a representative discussion of all measurement methods for the IFF approach. The CATR solution is based on the **R&S®ATS1800C** [Ref. 19].

4.1 Link and measurement angles

For dual-polarized measurement probe antennas and link antennas with different angles with respect to the DUT, the following definitions apply.

The **measurement angle** is the angle of measurement of the desired metric from the DUT's viewpoint. The **link angle** is the gNB emulator's downlink signal **angle of arrival (AoA)** from the DUT's viewpoint. In case of beam correspondence, the uplink signal **angle of departure (AoD)** is the same as the AoA within an allowed tolerance.

Two angles are of great interest for measurement purposes: The **TX beam peak direction** is the direction where the maximum total component of the **equivalent isotropic radiated power (EIRP)** is found. In other words, it is the AoD from the DUT's viewpoint with the strongest spatial power intensity emission. The **RX beam peak direction** is the direction where the maximum total **reference signal receive power (RSRP)** component and the best **equivalent isotropic sensitivity (EIS)** component are found. This corresponds to the AoA from the DUT's viewpoint with the best receiver sensitivity, i.e. the lowest directional reference sensitivity level.

Table 3 summarizes the link and measurement angle configurations for the different test metrics.

Table 3: Link and measurement angles

Link angle	Measurement angle	Test metrics
TX beam peak direction	Full sphere measurement grid	In beam lock mode using UBF: ► Maximum output power (TRP and EIRP) ► Minimum output power (EIRP) ► TX and RX spurious emissions (TRP) ► Spectrum emissions mask (TRP)
	Link angle	Without beam lock: ► Off power (TRP) ► Transmit on/off time mask (EIRP) ► Transmit signal quality (frequency error, EVM, carrier leakage, inband emissions, spectral flatness)
Beam peak search grids	Link angle	► UE minimum peak EIRP ► EIRP spherical coverage ► UE reference sensitivity ► EIS spherical coverage
RX beam peak direction	Link angle	► UE maximum input level (EIS) ► Adjacent channel selectivity (EIS) ► Inband blocking (EIS)

TX measurements are performed by measurement probes connected to the test setup signal analyzer (e.g. vector signal analyzer, power meter or gNB emulator). RX measurements are based on downlink throughput measurements or UE measurement reporting parameters, e.g. reference signal receive power (RSRP) or reference signal receive quality (RSRQ). The relevant test antenna is the link antenna, emitting the downlink signal towards the DUT and being connected to a base station emulator. Nevertheless, the link antenna and measurement probe may be combined as long as there are TX measurements in the link angle direction only.

4.2 Measurement requirements and assessment principles

Measurement requirements typically represent minimum values, i.e. they define common requirements to be met by all DUTs to ensure minimum performance. This allows network operators to plan and deploy cellular network structures based on minimum performance assumptions. In contrast, some minimum requirements are derived from regulatory requirements such as electromagnetic emission limits or spectral efficiency requirements.

By default, minimum requirements make no explicit allowance for **measurement uncertainties (MU)**. However, they must at least be reported in the test result documentation. **Test tolerances (TT)** may be used for certain tests to relax minimum requirements, e.g. by known measurement uncertainties due to given assessment principles.

ITU-R M.1545 specifies two popular assessment principles known as the **"never fail a good DUT or pass a bad one"** principle and the **"shared risk"** principle. The latter does not allow any test tolerances, i.e. the risk of wrong assessments is determined by measurement uncertainties only. It is the most popular principle for regulatory tests in particular. Assuming a symmetrical measurement uncertainty distribution (e.g. normal distribution) with respect to the true value, the risk of wrong assessments is equally "shared" between the device vendor and device consumer. In other words, the probability of failing a good DUT or passing a faulty one is equal and determined by the MU of the test setup. Consequently, the only way to minimize the total number of wrong assessments is to choose a test setup with the lowest possible MU, i.e. state-of-the-art T&M equipment.

In order to avoid failing a good DUT (or to prevent passing a bad one), a test tolerance equal to the MU can be added/deducted to/from the requirement limit. This principle may apply to selected requirements.

4.3 Environmental conditions

Conformance assessments must be performed under well-defined conditions that can include the environmental temperature and selected power supply conditions.

Normal temperature conditions are typically in the range from +15 °C to +35 °C, while extreme conditions extend the normal range as listed in Table 4. Different power supply conditions are also specified in order to ensure conformity under normal, low and high voltage conditions as listed in Table 5.

Table 4: Environmental temperature conditions according to 3GPP TS 38.508-1

	FR1	FR2
Normal conditions	+15 °C to +35 °C	+25 °C ± 10 °C
Extreme conditions	–10 °C to +55 °C	–10 °C to +55 °C

Table 5: Power supply conditions according to 3GPP TS 38.508-1

Power source	Lower extreme voltage	Higher extreme voltage	Normal voltage
AC mains	0.9 · nominal	1.1 · nominal	nominal
Regulated lead acid battery	0.9 · nominal	1.3 · nominal	1.1 · nominal
Non-regulated batteries			
Leclanché	0.85 · nominal	nominal	nominal
Lithium	0.95 · nominal	1.1 · nominal	1.1 · nominal
Mercury/nickel and cadmium	0.90 · nominal	1.1 · nominal	nominal

While specific supply voltage conditions can be provided to the DUT by appropriate DC power supplies, establishment of specific temperature conditions in an anechoic chamber requires dedicated equipment such as the R&S®CATR-TEMP2 bubble (see Figure 28). The purpose of this equipment is to regulate the space around the DUT with a type of air conditioning system. This includes controlled flow of dry air around the DUT at the desired temperature.

Figure 28: R&S®CATR-TEMP2 DUT enclosure for controlled environmental temperature conditions

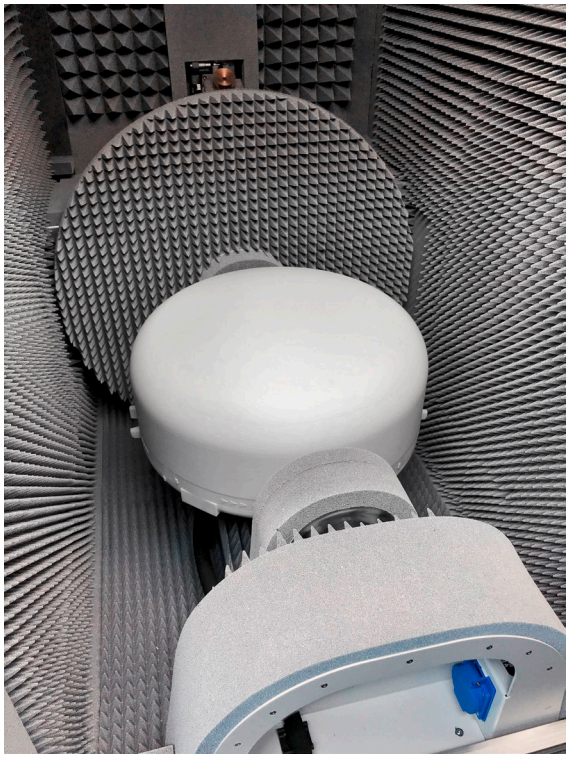

4.4 Preparatory OTA measurement procedures

As discussed so far, the DUT must be placed in the quiet zone of the OTA test setup. Dedicated calibration of the setup is necessary to ensure the required quality and size of the quiet zone and determine different measurement uncertainties. Since the calibration procedure is typically T&M vendor-specific, refer to the test setup calibration manual for details. Note that calibration procedures must follow 3GPP recommendations and satisfy the required measurement uncertainties. Given a calibrated environment, many preparatory OTA measurements are still required for each individual DUT. These preparatory measurements are necessary especially to identify the UE transmitter and receiver beam peak since some conformance metrics are specified in the beam peak direction only. Peak EIRP and EIS measurements are described in subsequent chapters. The TRP metric measurement procedure and transmit quality measurement procedure are also explained. Measurement of spurious emissions is a specific challenge that is covered in a separate chapter.

4.4.1 Initial DUT alignment

The DUT must be aligned based on the 3GPP reference coordinate system. There are three possible initial alignment options as shown in Figure 29.

Figure 29: DUT alignment options

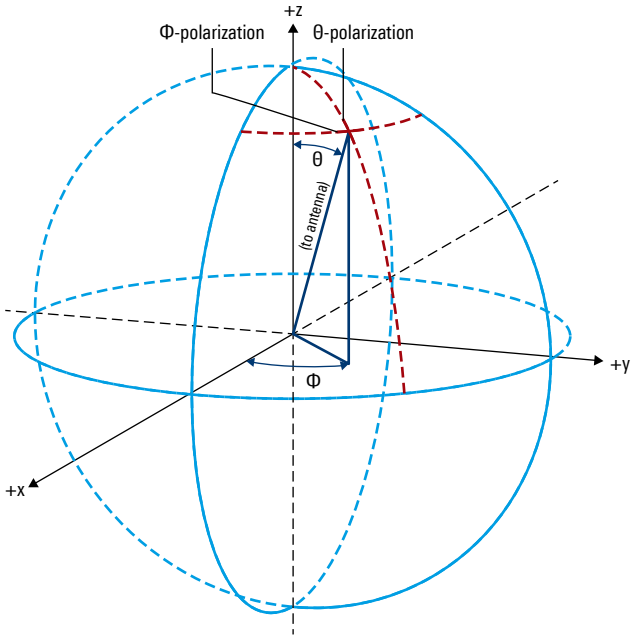

3GPP alignment reference coordinate system

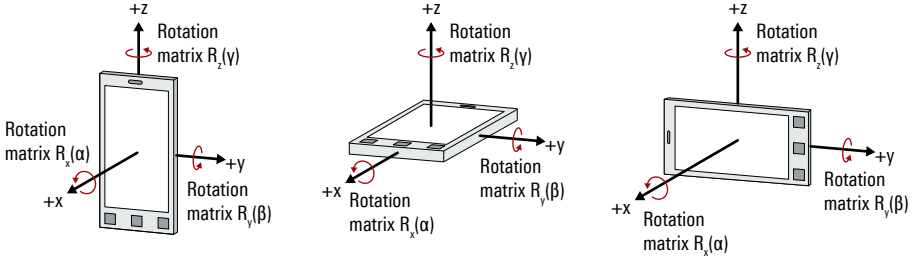

DUT orientation option 1 | DUT orientation option 2 | DUT orientation option 3

If the DUT needs to be manually rotated for a full sphere test (e.g. if the setup only covers half of the scan sphere), follow the realignment guidelines in 3GPP TR 38.810. For initial orientation, the rotation matrices ensure correct translation of results between Cartesian and polar coordinates with respect to the reference coordinate system.

4.4.2 TX beam peak direction search procedure

The DUT's TX beam peak direction is the direction of maximum total EIRP, including the polarization of the antenna used to measure the TX beam. The goal of the TX beam peak search is to find the total EIRP maximum. This includes the Θ and Φ polarization according to the reference coordinate system.

The beam peak search (which corresponds to the spherical coverage test procedure) may apply to DUTs with different beam correspondence capability as defined in 3GPP TS 38.306. To allow the DUT refocusing its TX beam using beam correspondence capability, the gNB emulator must ensure the presence of downlink reference signals, including both SSB and CSI-RS, and type D quasi co-location (QCL) must be maintained between SSB and CSI-RS [Ref. 7].

The TX beam peak direction is basically found with a 3D EIRP scan that is performed separately for each orthogonal polarization Θ and Φ using orthogonal measurement antennas. The TX beam peak direction search grid (e.g. 15° constant step size grid) according to 3GPP TS 38.810 applies (optionally using the coarse and fine grid approach).

Prior to total EIRP determination for each grid point, the link between the DUT and gNB emulator as part of the test system must be established via the measurement antenna with either link antenna polarization ($Pol_{Link} = \theta$ or $Pol_{Link} = \Phi$) to form the TX beam towards the selected measurement antenna. This means the link antenna is equal to the selected measurement antenna as shown in Figure 30.

Figure 30: Beam peak search procedure with combined link and measurement antennas

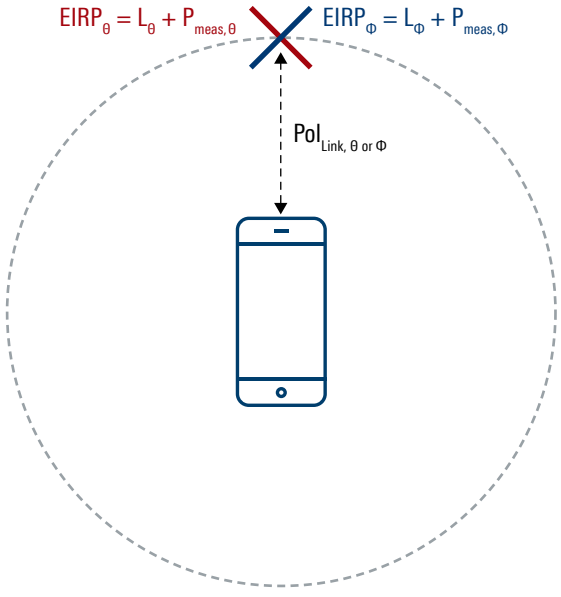

According to the DUT's beam correspondence capability (i.e. the ability of the UE to select a suitable beam for uplink transmission based on downlink measurements of both SSB and CSI-RS signals, as declared by the vendor), the TX beam is formed as follows:

Beam correspondence without relying on UL beam sweeping
The DUT autonomously chooses the TX beam direction based on measurements of the emulated downlink SSB and CSI-RS reference signals, i.e. towards the inverse direction of the incoming DL signal. This basically results in an angle of departure (AoD) that is equal to the angle of arrival (AoA) from the DUT's perspective within allowed tolerances.

Beam correspondence relying on network-assisted uplink beam sweeping
The DUT chooses the TX beam direction based on beam correspondence that relies on both downlink reference signals and network-assisted uplink beam sweeping.

The TX beam peak direction (Θ_{peak}, Φ_{peak}) is where the maximum total component of EIRP($Pol_{Link,\Theta}$) or EIRP($Pol_{Link,\Phi}$) is found. The individual EIRP samples are calculated by adding the composite path loss L_Θ and L_Φ, respectively, due to the free space path loss and test setup cabling based on the measured power P_{meas} as follows:

1. Measure mean power $P_{meas,\Theta}(Pol_{Link,\Theta})$
2. Calculate $EIRP_\Theta(Pol_{Link,\Theta}) = P_{meas,\Theta}(Pol_{Link,\Theta}) + L_\Theta$
3. Measure mean power $P_{meas,\Phi}(Pol_{Link,\Theta})$
4. Calculate $EIRP_\Phi(Pol_{Link,\Theta}) = P_{meas,\Phi}(Pol_{Link,\Theta}) + L_\Phi$
5. Calculate total $EIRP(Pol_{Link,\Theta}) = EIRP_\Theta(Pol_{Link,\Theta}) + EIRP_\Phi(Pol_{Link,\Theta})$

Repeat the total EIRP determination with switched link polarization, i.e. $Pol_{Link,\Phi}$.

This dual procedure must be repeated for each grid point. Finally, select the maximum EIRP value which indicates the TX beam peak direction (Θ_{peak}, Φ_{peak}).

During the individual power measurement scan, the DUT beam must be locked by means of UBF and the DUT must be continuously requested to transmit its maximum output power.

4.4.3 RX beam peak direction search procedure

The RX beam peak direction is the direction of the lowest sensitivity power level, i.e. the best equivalent isotropic sensitivity (EIS). The RX beam peak direction is determined with a 3D scan (separately for each orthogonal downlink polarization) while measuring the EIS power level.

The resulting average EIS is computed as the **harmonic mean** of both polarizations Θ and Φ according to the following equation.

Equation 1: Total EIS computation

$$EIS = \frac{2}{\frac{1}{EIS(\theta)} + \frac{1}{EIS(\phi)}}$$

Note: Receiver sensitivity EIS measures correspond to a certain SNR which allows a given minimum performance in terms of throughput (or error rate). Since the SNR is based on a ratio of the input signal power and the receiver noise floor, the mean EIS is calculated as a harmonic mean. Mathematically speaking, a harmonic mean is a type of numerical average. It is calculated by dividing the number of samples by the sum of the reciprocals of each sample in the series. Thus, the harmonic mean is the reciprocal of the arithmetic mean of the reciprocals. The harmonic mean is taken from the following general harmonic mean definition for H with N ratios of x:

$$H = \frac{N}{\sum_{i=1}^{N} \frac{1}{x_i}}$$

For the RX beam peak search, this measurement and the EIS computation are performed for a finite number of samples in a given grid. Typically, a constant step size grid with 30° steps in the elevation and azimuth directions is used. This results in 62 unique sampling points, assuming a single measurement at both poles. The RX beam peak corresponds to the angles (Θ_{peak}, Φ_{peak}) with the lowest sensitivity power level. Alternatively, the DUT's RSRP and RSRQ reports may be used to speed up the search procedure.

4.4.4 Spherical coverage

Spherical coverage requirements are exclusive to OTA assessments. There is no such metric for conducted measurements. For instance, the spherical coverage of a handheld device is a critical parameter for mobile communications systems because the angle of incoming signals and the UE orientation are generally random. Therefore, a statistical approach is used for spherical coverage requirements. For a certain percentile of directions (i.e. a certain part of the sphere around the UE), the transmitter and receiver must fulfill certain requirements. While a transmitter's spherical coverage is related to its EIRP pattern, a receiver's spherical coverage is related to its EIS pattern.

The uplink spherical coverage of a UE is evaluated by the CDF of EIRP in FR2. The CDF of a UE's EIRP can be calculated as CDF(eirp) = P(EIRP(Θ_i, Φ_j) ≤ eirp). Note that the right-hand side of this equation represents the probability that the measured EIRP(Θ_i, Φ_j) takes on a value less than or equal to a threshold eirp value.

For a given CDF of a series of EIRP measurements, the EIRP value at CDF = 0% indicates the minimum EIRP. The value when CDF = 100% indicates the peak EIRP value. 3GPP defines four 5G FR2 device power classes. The mobile handset type UE (e.g. a smartphone) is categorized as power class 3 (PC3). For PC3, both the peak EIRP value and the spherical coverage performance are critical. The **minimum peak EIRP** value represents UE beamforming capability measured by the EIRP value at CDF = 100%. Requirements are met if the UE exceeds the limit in one direction (beam peak). The requirement for spherical coverage in PC3 is specified at CDF = 50%. This is known as the minimum EIRP at **50%ile CDF**. The requirements for the different power classes are listed in Table 9 to Table 12.

We will now consider a full sphere EIRP(Θ_i, Φ_j) scan using a 15° constant step size grid, resulting in 266 measurements as described in the following figure.

Figure 31: Metrics for transmitter spherical coverage assessment

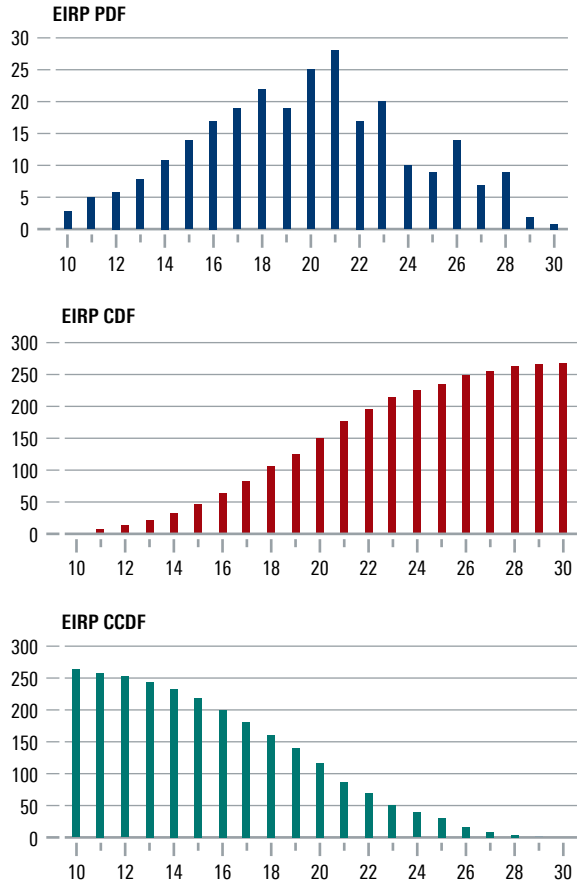

The PDF of a series of EIRP(Θ_i, Φ_j) measurements illustrates the frequency of the measurement values. This example depicts a spread of EIRP levels between 10 dBm and 30 dBm. In total, there were 266 measurements in this example. EIRP = 20 dBm was measured 25 times. In other words, 25/266 = 9.3 % of all measurements were exactly 20 dBm.

The CDF of the same series of EIRP(Θ_i, Φ_j) measurements illustrates the accumulated frequency of the measurement values across the entire dynamic range of the values. For instance, EIRP less than or equal to 20 dBm was measured 149 times according to the EIRP CDF. In other words, 149/266 = 56 % of all EIRP measurements did not exceed 20 dBm.

The CCDF of the same series of EIRP(Θ_i, Φ_j) measurements illustrates the complementary accumulated frequency of the measurement values across the entire dynamic range of the values. For instance, EIRP greater than 20 dBm was measured 117 times according to the EIRP CCDF. In other words, 117/266 = 44 % of all EIRP measurements exceeded 20 dBm.

The downlink spherical coverage of the UE is evaluated by the CCDF of EIS. The CCDF of the UE EIS can be calculated as CCDF(**eis**) = P(EIS(Θ_i, Φ_j) > **eis**). The right-hand side of this equation represents the probability that the measured EIS(Θ_i, Φ_j) takes on a value greater than a threshold eis value. Power class specific downlink spherical coverage requirements are listed in Table 15.

Note:
Mathematical definition of the cumulative distribution function:

$$CDF(x) = P(X \leq x) = \int_{-\infty}^{x} PDF(X)dX$$

CDF(x) for a given random series X, e.g. a series of EIRP measurements, represents the probability that the measured values will not exceed a certain limit x.

Mathematical definition of the complementary cumulative distribution function:

$$CCDF(y) = 1 - CDF(y) = P(Y > y) = \int_{y}^{\infty} PDF(Y)dY$$

CCDF(y) for a given random series Y, e.g. a series of EIS measurements, represents the probability that the measured values exceed the limit y.

4.4.5 TRP measurement

The total radiated power can be determined by performing an OTA measurement of the transmit antenna feed power. This is equivalent to the conducted output power measurement when deducting the mismatch and efficiency of the connected antennas. To prevent distortion of the TRP result, beam adjustment must be avoided during the measurement. This is possible with the UE beam lock function (UBF) through signaling in preparation for the TRP measurement. The TRP measurement setup is illustrated in Figure 32.

Figure 32: TRP procedure with independent link and measurement antennas

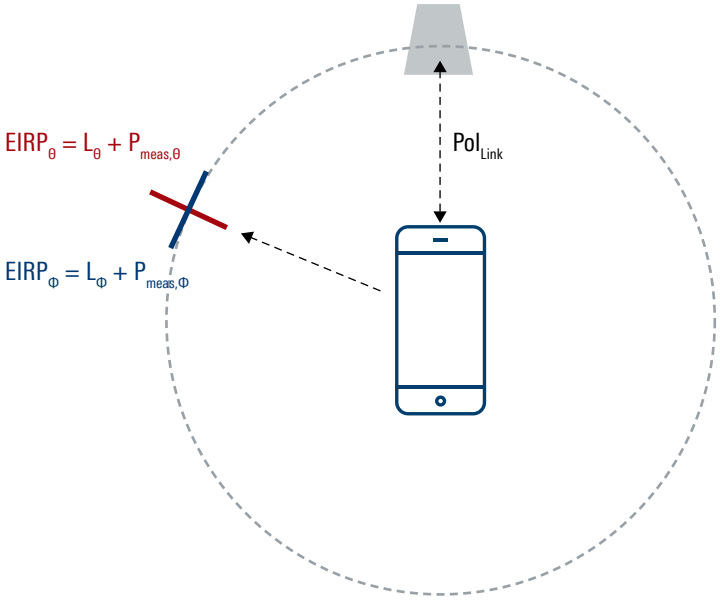

Since we can only scan the full sphere with a finite number of samples, specified search grids apply. These grids were defined to ensure a reasonable measurement uncertainty with a minimum of samples while avoiding excessive measurement times. Both grid types (constant step size and constant density) were considered. Obviously, a grid with a finite number of samples results in a systematic measurement uncertainty that can be reduced by increasing the number of samples. Typically, a constant step size grid with 15° steps in the elevation and azimuth directions results in 266 unique sampling points, assuming a single measurement at both poles. This results in a systematic measurement error of 0.65 dB according to simulation results provided in 3GPP TS 38.810. For instance, reducing the systematic error to less than 0.1 dB would require a constant step size of 5°, thereby entailing 2522 measurements. Higher accuracy comes at the cost of a 10-fold increase in measurement time. Clearly, OTA measurements always involve a tradeoff between accuracy and test time.

4.5 Inband transmitter characteristics

FR2 transmitter characteristics are specified over the air (OTA) with a single or multiple transmit chain(s). The identified beam peak direction can be stored and reused if it does not change according to the vendor's declaration. The channel bandwidth should be prioritized in the selection of test points. The subcarrier spacing (60 kHz or 120 kHz) should be selected after the test channel bandwidth is chosen. The DUT should also disable any UL TX diversity schemes for conformance testing.

Four different UE power classes for FR2 operation are defined by the 3GPP as listed in Table 7.

Table 7: FR2 UE power classes

UE power class	UE type
PC 1 (35 dBm TRP)	Fixed wireless access (FWA) UE
PC 2 (23 dBm TRP)	Vehicular UE
PC 3 (23 dBm TRP)	Handheld UE
PC 4 (23 dBm TRP)	High-power non-handheld UE

Table 8 gives an overview of all UE transmitter test topics. Transmitter test cases are specified in TS 38.521-2 subclause 6. Tests are specified for single carrier operation by default. Carrier aggregation related tests are specified in dedicated subclauses denoted as 6.x**A**. UL MIMO related test cases are specified in subclauses 6.x**D**. However, not all transmitter test cases have been fully specified at this time. The table reflects the status in line with TS 38.521-2 V16.6.0.

Table 8: FR2 UE transmitter test topics

3GPP TS 38.521-2 reference	Transmitter test topics
6.2, 6.2A (CA), 6.2D (UL MIMO)	UE transmit power, incl. maximum output power, output power reduction, output power with additional requirements and configured output power
6.3, 6.3A (CA), 6.3D (UL MIMO)	UE output power dynamics, incl. minimum output power, off power, on/off time mask and power control
6.4, 6.4A (CA), 6.4D (UL MIMO)	UE transmit signal quality, incl. frequency error and modu-lation quality (EVM, carrier leakage, inband emissions and equalizer spectrum flatness)
6.5, 6.5A (CA), 6.5D (UL MIMO)	UE output RF spectrum emissions, incl. occupied band-width, out of band and spurious emissions
6.6, 6.6A (CA)	Beam correspondence

4.5.1 UE output power requirements

The following UE output power metrics are tested for conformity:

UE minimum peak EIRP (in dBm)

This is the minimum peak EIRP required and is a lower limit without tolerance.

UE maximum peak EIRP (in dBm)

This is the maximum peak EIRP allowed and is an upper limit without tolerance derived from regulatory requirements.

UE maximum TRP

TRP is measured with the UE beam locked under normal conditions. It corresponds to the conducted transmit power fed to the transmit antenna. TRP is the only OTA power metric that can be directly related to a conducted power metric.

UE spherical coverage: minimum EIRP at n-th percentile CDF (in dBm)
This is a lower limit without tolerance tested under normal conditions only.

The minimum power measurement duration is equal to at least one time slot. The limits apply for any transmission bandwidth and should be tested at low, middle and high range carrier frequencies for DFT-s-OFDM QPSK with 120 kHz SCS.

Power class 1 output power limits are listed in Table 9, power class 2 in Table 10, power class 3 in Table 11 and power class 4 in Table 12. Note that for power class 2, frequency band n260 is not specified.

Table 9: UE power class 1 output power limits

FR2 operating band	Minimum peak EIRP	Maximum (minimum) EIRP	Maximum TRP	Minimum EIRP at 85 %ile CDF
n257	40 dBm	55 (4) dBm	35 dBm	32 dBm
n258	40 dBm	55 (4) dBm	35 dBm	32 dBm
n260	38 dBm	55 (4) dBm	35 dBm	30 dBm
n261	40 dBm	55 (4) dBm	35 dBm	32 dBm

Table 10: UE power class 2 output power limits
(Note: n260 not available for power class 2)

FR2 operating band	Minimum peak EIRP	Maximum (minimum) EIRP	Maximum TRP	Minimum EIRP at 60 %ile CDF
n257	29 dBm	43 (–13) dBm	23 dBm	18 dBm
n258	29 dBm	43 (–13) dBm	23 dBm	18 dBm
n261	29 dBm	43 (–13) dBm	23 dBm	18 dBm

Table 11: UE power class 3 output power limits

FR2 operating band	Minimum peak EIRP	Maximum (minimum) EIRP	Maximum TRP	Minimum EIRP at 50 %ile CDF
n257	22.4 dBm	43 (–13) dBm	23 dBm	11.5 dBm
n258	22.4 dBm	43 (–13) dBm	23 dBm	11.5 dBm
n260	20.6 dBm	43 (–13) dBm	23 dBm	8 dBm
n261	22.4 dBm	43 (–13) dBm	23 dBm	11.5 dBm

Table 12: UE power class 4 output power limits.

FR2 operating band	Minimum peak EIRP	Maximum (minimum) EIRP	Maximum TRP	Minimum EIRP at 20 %ile CDF
n257	34 dBm	43 (–13) dBm	23 dBm	25 dBm
n258	34 dBm	43 (–13) dBm	23 dBm	25 dBm
n260	31 dBm	43 (-13) dBm	23 dBm	19 dBm
n261	34 dBm	43 (–13) dBm	23 dBm	25 dBm

The different power classes have different output power and spherical coverage limits due to the different transmit antenna directivity requirements. For example, power class 3 for typical handheld devices requires good mean coverage (50 %ile minimum EIRP requirement, i.e. half the transmit sphere may exceed the minimum limit). In contrast, power class 1 devices for fixed radio link connections are designed for high directivity (i.e. small half-power beamwidth) towards the base station, resulting in an 85 %ile minimum EIRP requirement. Thus, only 15 % of the sphere may exceed the limit.

4.5.2 Transmit signal quality requirements

Different parameters are used to characterize the transmit signal quality as listed below. In general, signal quality measurements involve comparisons with an ideally modulated signal, except for the frequency error. The frequency error is the offset to the actual downlink signal carrier frequency that serves as the UE transmitter reference during the measurement.

Frequency error

The UE modulated carrier frequency should be accurate to ±0.1 ppm compared to the downlink carrier frequency.

Error vector magnitude (EVM)

EVM is the difference between the measured and reference waveform after frequency and timing offset correction. It is expressed as the magnitude of the difference (error vector) of the measured and reference signal vector with respect to the magnitude of the reference signal vector. Allowed values are listed in Table 13.

EVM equalizer spectrum flatness

Quality of the equalizer coefficients in order to create a flat spectrum within the occupied band.

Carrier leakage

Carrier leakage is defined as the unmodulated sine wave with the carrier frequency expressed as a relative level (dBc).

Inband emissions for non-allocated resource blocks

Measure of the inherent interference falling into the non-allocated resource blocks.

Table 13: EVM conformance levels

Modulation scheme	Average EVM level	Reference signal EVM level
$\pi/2$ BPSK	30% (–10.5 dB)	30% (–10.5 dB)
QPSK	17.5% (–15.1 dB)	17.5% (–15.1 dB)
16QAM	12.5% (–18 dB)	12.5% (–18 dB)
64QAM	8% (–22 dB)	8% (–22 dB)

Note that all transmit signal quality tests are performed in beam locked mode in the beam peak direction and for both polarizations on the UL. Transmit signal quality measurements are performed using the global in-channel TX test method in line with 3GPP. The corresponding signal quality measurement points are illustrated in Figure 33.

Figure 33: Signal quality measurement points (source: 3GPP TS 38.521-2)

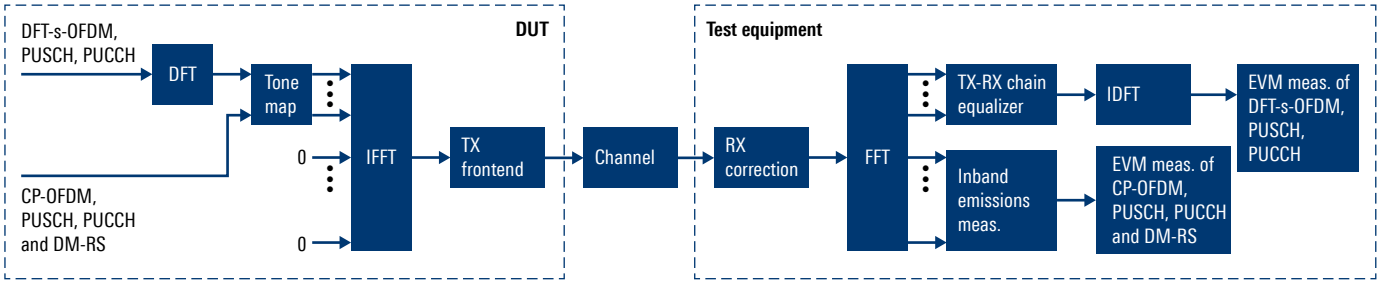

Test equipment basically demodulates the DUT transmit signal, including high-quality downconversion and RF correction (which determines the frequency error and carrier leakage) prior to the measurement receiver FFT stage. After the FFT stage, allocated and

non-allocated resource blocks (subcarriers over time) are available. Unwanted emissions falling into non-allocated resource blocks (inband emissions measurement) can be calculated directly after the initial FFT stage. The allocated subcarriers are fed to a best practice equalizer which provides all residual metrics such as EVM and spectral flatness for the CP-OFDM type of transmit signals. An IDFT stage in the measurement receiver is needed to fully analyze DFT-s-OFDM test signals.

4.6 Output RF spectrum emission requirements

The transmitter output RF spectrum emission frequency ranges are summarized in Figure 34. Starting at the wanted signal carrier frequency f_c, there is an inband parameter known as the occupied bandwidth (OBW). It contains 99 % of the wanted transmit power. The range $f_c \pm 2.5$ OBW is known as the out-of-band range, including the adjacent channels. The adjacent channels are also covered by the adjacent channel leakage power (ACLP), which is also known as the adjacent channel leakage ratio (ACLR) or adjacent channel power (ACP). Beyond that range comes the spurious emissions (SE) range. This range is of special interest to regulators who are tasked with protecting other radio services from spurious emissions. Spurious emissions ranges and limits are listed in Table 14 for the USA (FCC) and Europe (CEPT).

Figure 34: Transmitter output emission ranges

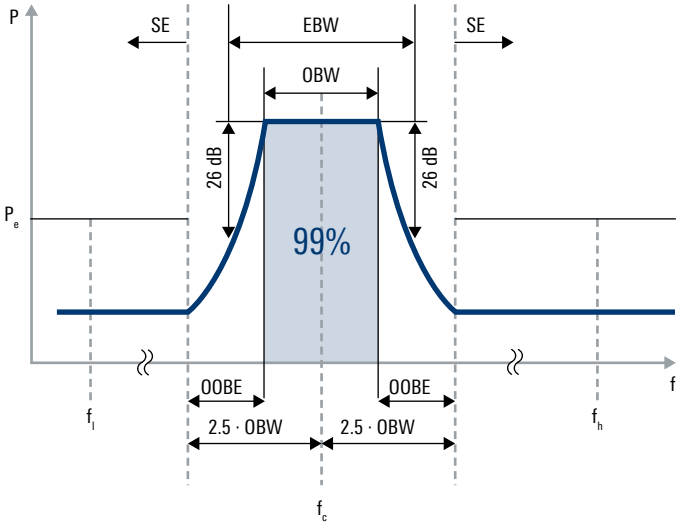

3GPP output RF spectrum emissions testing covers three major parts including subparts:

- Occupied bandwidth (OBW)
- Out-of-band emissions (OOBE) including
  - Spectrum emission mask (SEM) within emission bandwidth (EBW)
  - Adjacent channel leakage ratio (ACLR)
- Transmitter (and receiver) spurious emissions

Table 14: International spurious emissions ranges and limits (USA and EU)

f_c	f_l	f_h	P_e
USA			
9 kHz to 10 GHz	9 kHz	$10 f_c$ or 40 GHz	–13 dBm (1 MHz)
10 GHz to 30 GHz	9 kHz	$5 f_c$ or 100 GHz	–13 dBm (1 MHz) or 1% EBW
> 30 GHz	9 kHz	$5 f_c$ or 200 GHz	–13 dBm (1 MHz) or 1% EBW
EU			
9 kHz to 100 MHz	9 kHz	1 GHz	–36 dBm (100 kHz)
100 MHz to 300 MHz	9 kHz	$10 f_c$	–36 dBm (100 kHz)
300 MHz to 600 MHz	30 MHz	3 GHz	–36 dBm (100 kHz)
600 MHz to 1 GHz	30 MHz	$5 f_c$	–36 dBm (100 kHz)
1 GHz to 5.2 GHz	30 MHz	$5 f_c$	–30 dBm (1 MHz)
5.2 GHz to 7.25 GHz	30 MHz	26 GHz	–30 dBm (1 MHz)
> 7.25 GHz	30 MHz	$2 f_c$	–13 dBm (1 MHz) and –10 dBm (100 MHz)

Note: Regulatory requirements are subject to regional variations. Be sure to verify the latest requirements with the regulator in your region of interest.

4.7 Receiver characteristics

Receiver characteristics are measured in terms of throughput. Throughput is a measure of successfully received user data per time interval, e.g. bits per second (bps). The conformance requirement for receivers is generally a minimum throughput at specified receiver input levels depending on the modulation and coding scheme and the radio channel profile. These parameters are specified in terms of **reference measurement channels (RMC)**. Therefore, a UE's **receiver sensitivity** is defined as the **minimum receive power level** required to provide a data throughput rate greater than or equal to 95% of the maximum possible throughput of a given RMC.

The assumption that all subscriber UEs in the field meet this minimum performance requirement is the basis for radio network planning, e.g. determination of the effective coverage area for each radio base station. Consequently, minimum performance conformance measurements are carried out by measuring the throughput at the 3GPP's specified reference sensitivity level $P_{REFSENS}$. Well-defined reference channel configurations are used to ensure traceability, repeatability and comparability of the measurements.

A UE meets conformance requirements as long as the measured throughput is ≥ 95% of the maximum possible throughput while receiving data at the reference sensitivity level. The reference measurement channels (RMC) are composed of the modulation and coding scheme (MCS) provided for user data transmission and the physical resource block (PRB) allocation, which includes the available channel bandwidth (BW). Higher order MCS provides greater spectral efficiency (bits per second and per hertz), but at the cost of a higher reference sensitivity level. In other words, greater throughput is not free because it entails a reduction in coverage.

The following aspects are relevant for receiver conformance testing:

- The focus is on the receiver's ability to demodulate and decode a wanted signal with a specified modulation and coding scheme with (selectivity) or without (sensitivity) the presence of unwanted signals
- Receiver sensitivity is verified by measuring user data throughput at a specified reference power level
- Metrics like EIS allow verification of receiver sensitivity from a spatial perspective
- In contrast to the minimum receiver sensitivity, the maximum input metric involves verification of the receiver performance at very high input levels

- Receiver selectivity is verified by measuring user data throughput at a specified unwanted (e.g. adjacent channel signal or blocking signal) to wanted signal power ratio
- Basic receiver sensitivity and selectivity tests are performed under static propagation conditions for both wanted and unwanted signals
- The throughput should be ≥ 95 % of the maximum possible throughput at the reference power level
- Advanced receiver sensitivity and selectivity tests are performed under simulated multipath channel conditions, e.g. for testing receiver characteristics using MIMO schemes

4.7.1 OTA receiver sensitivity power level

The receiver sensitivity power level $P_{REFSENS}$ is determined by the noise power P_{noise} at the output of the receiver's low noise amplifier. This is given by the following equation.

Equation 2: Receiver output noise power

$$P_{noise}\ (in\ dB) = 10 \cdot \log_{10}(k \cdot T) + 10 \cdot \log_{10}(BW) + NF$$

- k: Boltzmann constant ($1.38 \cdot 10^{-23}$ J/K)
- T: System temperature
- BW: Signal or channel bandwidth
- NF: UE receiver's noise figure in dB

The factor $10\log_{10}(k \cdot T)$, known as the spectral noise power density $N_{0,}$ is typically set to –174 dBm (1 Hz), which assumes a system temperature of T = 290 K. The bandwidth factor $10\log_{10}(BW)$ accumulates the spectral noise power density across the channel bandwidth of interest. For instance, 100 MHz bandwidth contributes a bandwidth factor of 80 dB, resulting in noise power N = –94 dBm. The noise figure (NF) is UE implementation specific, i.e. it ultimately determines the quality of the actual UE receiver. Typical values are in the range from 8 dB to 12 dB.

Now, for each modulation and coding scheme (MCS), a minimum signal-to-noise (SNR) ratio is required in order to ensure the minimum required performance (e.g. 95 % of the maximum possible throughput for the given MCS). Thus, the reference sensitivity level $P_{REFSENS}$ of a receiver for a certain MCS is as follows.

Equation 3: Reference sensitivity level

$$P_{REFSENS} = P_{noise} + SNR_{min}(MCS)$$

Finally, the radiated performance is what counts in real operation (and especially for assessment of FR2 devices). By extending Equation 3, this is expressed by the following directional reference sensitivity.

Equation 4: Directional reference sensitivity level

$$P_{REFSENS}(\theta, \Phi) = P_{noise} + SNR_{min}(MCS) - G(\theta, \Phi)$$

Here, $G(\Theta, \Phi)$ represents the spatial selective receive antenna gain.

The reference sensitivity level decreases (i.e. the receiver becomes more sensitive) as the receiver's antenna gain increases. In other words, **the receiver's highest sensitivity is in its antenna beam peak direction**. Accordingly, receiver performance should be tested in the beam peak direction (Θ_{max}, Φ_{max}). This parameter is determined using the dedicated receiver beam peak search procedure (see chapter 3.4.3).

Based on simulations and manufacturer input, the 3GPP assumes certain NF values and receive antenna gains in order to set conformance reference sensitivity power levels. [Ref. 2] provides $P_{REFSENS}$ values for different frequency ranges, bandwidths and modulation schemes. For example, Table 15 shows some of the requirements for the QPSK modulation scheme.

Note that the values increase with increasing order of modulation and coding scheme. This corresponds to the increase in SNR_{min}(MCS) in Equation 3.

Table 15: UE receiver OTA reference sensitivity power levels in beam peak direction

–	50 MHz	100 MHz	200 MHz	400 MHz
Power class 1: fixed wireless access (FWA) UE				
n257	–97.5 dBm	–94.5 dBm	–91.5 dBm	–88.5 dBm
n258	–97.5 dBm	–94.5 dBm	–91.5 dBm	–88.5 dBm
n260	–94.5 dBm	–91.5 dBm	–88.5 dBm	–88.5 dBm
n261	–97.5 dBm	–94.5 dBm	–91.5 dBm	–88.5 dBm
Power class 2: vehicular UE				
n257	–94.5 dBm	–91.5 dBm	–88.5 dBm	–85.5 dBm
n258	–94.5 dBm	–91.5 dBm	–88.5 dBm	–85.5 dBm
n260	N/A	N/A	N/A	N/A
n261	–94.5 dBm	–91.5 dBm	–88.5 dBm	–85.5 dBm
Power class 3: handheld UE				
n257	–88.3 dBm	–85.3 dBm	–82.3 dBm	–79.3 dBm
n258	–88.3 dBm	–85.3 dBm	–82.3 dBm	–79.3 dBm
n260	–85.7 dBm	–82.7 dBm	–79.7 dBm	–76.7 dBm
n261	–88.3 dBm	–85.3 dBm	–82.3 dBm	–79.3 dBm
Power class 4: high-power non-handheld UE				
n257	–97 dBm	–94 dBm	–91 dBm	–88 dBm
n258	–97 dBm	–94 dBm	–91 dBm	–88 dBm
n260	–95 dBm	–92 dBm	–89 dBm	–86 dBm
n261	–97 dBm	–94 dBm	–91 dBm	–88 dBm

4.7.2 Equivalent isotropic sensitivity (EIS)

EIS measurements are OTA receiver performance measurements from a given direction (Θ, Φ), e.g. directive BLER or throughput measurements. Thus, analogous to EIRP based transmit radiation pattern measurements, an EIS based receive radiation pattern measurement is possible, e.g. to determine the receiver's beam peak.

With the EIS metric throughput, the reference sensitivity EIS for a certain AoA (Θ, Φ) is found by lowering the UE input power from direction (Θ, Φ) as long as the throughput remains above 95 % of the maximum possible throughput for the MCS under test. The corresponding power level at the 95 % throughput threshold represents the receiver's **directional sensitivity power level** for that direction (Θ, Φ). Finally, the direction with the lowest power level represents the receive antenna beam peak direction $(\Theta_{max}, \Phi_{max})$.

Furthermore, a statistical assessment of the directional EIS(Θ, Φ) can be performed. This is known as the receiver spherical coverage. Basically, a minimum sensitivity is required in a certain number of directions.

Table 16: UE receiver spherical coverage requirements

–	50 MHz	100 MHz	200 MHz	400 MHz
Power class 1: fixed wireless access (FWA) UE, EIS at 85 %ile CCDF				
n257	–89.5 dBm	–86.5 dBm	–83.5 dBm	–80.5 dBm
n258	–89.5 dBm	–86.5 dBm	–83.5 dBm	–80.5 dBm
n260	–86.5 dBm	–83.5 dBm	–80.5 dBm	–77.5 dBm
n261	–89.5 dBm	–86.5 dBm	–83.5 dBm	–80.5 dBm
Power class 2: vehicular UE, EIS at 60 %ile CCDF				
n257	–83.5 dBm	–80.5 dBm	–77.5 dBm	–74.5 dBm
n258	–83.5 dBm	–80.5 dBm	–77.5 dBm	–74.5 dBm
n260	N/A	N/A	N/A	N/A
n261	–83.5 dBm	–80.5 dBm	–77.5 dBm	–74.5 dBm
Power class 3: handheld UE, EIS at 50 %ile CCDF				
n257	–77.4 dBm	–74.4 dBm	–71.4 dBm	–68.4 dBm
n258	–77.4 dBm	–74.4 dBm	–71.4 dBm	–68.4 dBm
n260	–73.1 dBm	–70.1 dBm	–67.1 dBm	–64.1 dBm
n261	–77.4 dBm	–74.4 dBm	–71.4 dBm	–68.4 dBm
Power class 4: high-power non-handheld UE, EIS at 20 %ile CCDF				
n257	–88 dBm	–85 dBm	–82 dBm	–79 dBm
n258	–88 dBm	–85 dBm	–82 dBm	–79 dBm
n260	–83 dBm	–80 dBm	–77 dBm	–74 dBm
n261	–88 dBm	–85 dBm	–82 dBm	–79 dBm

Table 16 shows the receiver spherical coverage requirements for different UE power classes with different directional requirements. For instance, the n260 FR2 band power class 3 handheld UE should meet the EIS 50 %ile CCDF limit at an input level of –70.1 dBm for a 100 MHz signal. In other words, for at least half of the possible angles of arrival (assuming a full sphere), the receiver's sensitivity level should be less than or equal to –70.1 dBm. This value is in contrast to the peak reference sensitivity level for that case of –82.7 dBm according to Table 16. The latter value represents the "best possible" sensitivity the receiver must offer for a certain (beam peak) direction. The spherical coverage sensitivity, however, is a measure of the "experienced" sensitivity in any direction.

For highly directive power class 1 FWA devices, the required spherical coverage sensitivity level is much lower (i.e. better) than for power class 3 devices. For example, this value is 13 dB lower for the same FR2 band and bandwidth compared to the power class 3 example. However, this is the 85 %ile CCDF limit, meaning this limit should be met only for at least 15 % of all directions. Since an FWA device is installed once with its beam peak towards the incoming signal and is not moved thereafter, wider spherical coverage is obviously not as critical as in the case of a handheld or other type of device.

Note that the EIS(Θ, Φ) measurement results acquired while searching for the receiver beam peak can also be used for statistical spherical coverage assessment.

4.7.3 Receiver assessment metrics

Finally, we can summarize the receiver conformance assessment metrics specified by the 3GPP:

Reference sensitivity power level (in dBm)

The reference sensitivity power level $P_{REFSENS}$ is the EIS level at the center of the quiet zone in the RX beam peak direction. The throughput should meet or exceed the requirements for the specified reference measurement channel. The reference receive sensitivity is defined assuming a 0 dBi reference antenna located at the center of the quiet zone.

EIS spherical coverage (N %ile CCDF EIS power level in dBm)

The N %ile CCDF specifies the sensitivity level threshold.

Maximum input level

Equal to –25 dBm for all bandwidths, this is the maximum input level a receiver should tolerate without any performance degradation.

Adjacent channel selectivity (ACS)

ACS represents the UE's ability to receive data with a given average throughput on a reference measurement channel in the presence of an adjacent channel signal at a given frequency offset from the center frequency of the assigned channel.

Inband blocking

Inband blocking is defined for an unwanted interfering signal falling into the UE receive band or into spectrum equivalent to twice the channel bandwidth below or above the UE receive band. The relative throughput should meet or exceed the minimum requirement for the specified measurement channels.

Table 17 provides an overview of UE receiver test topics. Test cases are specified in TS 38.521-2 subclause 7. Tests are specified for single carrier operation by default. Carrier aggregation related tests are specified in dedicated subclauses denoted as 7.x**A**. UL MIMO related test cases are specified in subclauses 7.x**D**. However, not all receiver test cases have been fully specified at this time. The table reflects the status according to TS 38.521-2 V16.6.0.

Table 17: FR2 UE receiver test topics

3GPP TS 38.521-2 reference	Receiver test metric
7.3, 7.3A (CA), 7.3D (UL MIMO)	Reference sensitivity incl. reference sensitivity power level and EIS spherical coverage
7.4, 7.4A (CA), 7.4D (UL MIMO)	Maximum input level
7.5, 7.5A (CA), 7.5D (UL MIMO)	Adjacent channel selectivity (ACS)
7.6, 7.6D (UL MIMO)	Blocking characteristics incl. inband blocking only

5 REFERENCES

[Ref. 1] C. A. Balanis, Antenna Theory, Wiley & Sons editor, 2005

[Ref. 2] IEEE, IEEE standard test procedures for antennas, IEEE Std. 149-1979, 1979

[Ref. 3] IEEE, IEEE standard for definitions of terms for antennas, IEEE Std. 145, 2013

[Ref. 4] M. Reil, G. Lloyd, Millimeterwave Beamforming: Antenna Array Design Choices & Characterization (1MA276), Rohde & Schwarz white paper, 2016, www.rohde-schwarz.com/appnote/1MA276

[Ref. 5] M. Kottkamp, C. Rowell, Antenna Array Testing – Conducted and Over the Air: The Way to 5G (1MA286) Rohde & Schwarz white paper, 2017, www.rohde-schwarz.com/appnote/1MA286

[Ref. 6] A. Naehring, Over the Air Testing: Important Antenna Parameters, Testing Methodologies and Standards Rohde & Schwarz article, 2018, www.rohde-schwarz.com/us/solutions/test-and-measurement/wireless-communication/wireless-5g-and-cellular/5g-test-and-measurement/ota-whitepaper_251028.html (registration required)

[Ref. 7] M. Kottkamp, A. Pandey, D. Raddino, A. Roessler, R. Stuhlfauth, 5G NR fundamentals, procedures and test aspects, Rohde & Schwarz technology book, 2019, paperback or electronic eBook on www.rohde-schwarz.com/5G

[Ref. 8] C. Wicke, F. Bette, 5G New radio over-the-air base station transmitter tests (GFM324), Rohde & Schwarz application note, 2020, www.rohde-schwarz.com/appnote/GFM324

[Ref. 9] C. Wicke, F. Bette, 5G New radio over-the-air base station receiver tests (GFM325), Rohde & Schwarz application note, 2020, www.rohde-schwarz.com/appnote/GFM325

[Ref. 10] S. A. Schelkunoff, H.T. Friis, Antenna theory and practice, Wiley, New York, 1952

[Ref. 11] G. Pfeiffer, Five things you need to know about OTA chambers for 5G NR mmWave testing, Rohde & Schwarz webinar, 2020, www.rohde-schwarz.com/de/knowledge-center/webinars/ota-chambers-for-5g-nr-mmw-testing_252672.html (registration required)

[Ref. 12] A. D. Yaghjian, An overview of near-field antenna measurements, IEEE AP-34, 1986

[Ref. 13] IEEE, IEEE Recommended Practice for Near-Field Antenna Measurements, IEEE 1720, 2012

[Ref. 14] Z. Chen, V. Rodriguez, Proposed Changes and Updates on IEEE Std 1128 – Recommended Practice on Absorber Evaluation, published in Antenna Measurement Techniques Association Symposium (AMTA), San Diego, CA, USA, 2019, https://ieeexplore.ieee.org/document/8906362

[Ref. 15] R&S®ATS1000 Antenna Test System, Rohde & Schwarz product brochure, PD 5214.7170.12, Version 02.00, October 2018, can be downloaded from the Rohde & Schwarz webpage www.rohde-schwarz.com/product/ats1000

[Ref. 16] Over-the-air (OTA) testing fundamentals, Rohde & Schwarz poster, PD 5216.4162.82, Version 01.00, February 2019, can be downloaded (registration required) from the Rohde & Schwarz webpage www.rohde-schwarz.com/solutions/test-and-measurement/wireless-communication/wireless-5g-and-cellular/5g-test-and-measurement/ota-poster_250660.html

[Ref. 17] B. Derat, 5G Antenna Characterization in the Far Field: How close can Far-Field be?, published in IEEE International Symposium on Electromagnetic Compatibility and IEEE Asia-Pacific Symposium on Electromagnetic Compatibility (EMC/APEMC), Suntec City, Singapore, 2018, https://ieeexplore.ieee.org/document/8393926

[Ref. 18] B. Derat, C. Rowell, A. Tankielun, Promises of Near-Field Software and Hardware Transformations for 5G OTA, published in IEEE Conference on Antenna Measurements & Applications (CAMA), Västerås, Sweden, 2018, https://ieeexplore.ieee.org/document/8530646

[Ref. 19] R&S®ATS1800C CATR Based Compact 5G NR mmWave Test Chamber, Rohde&Schwarz product flyer, PD 3608.1298.32, Version 01.00, October 2019, can be downloaded from the Rohde&Schwarz webpage www.rohde-schwarz.com/product/ats1800C

[Ref. 20] M. Reckeweg, C. Rohner, Antenna Basics (8GE01), Rohde&Schwarz white paper, 2015, www.rohde-schwarz.com/appnote/8GE01

Note: All links have been checked and were functional when this document was created. However, we cannot rule out subsequent changes to the links in the reference list.

6 LIST OF ABBREVIATIONS

Term	Explanation
AAS	Active antenna system
AC	Anechoic chamber
ACLR	Adjacent channel leakage ratio
ACS	Adjacent channel selectivity
AoA	Angle of arrival
AoD	Angle of departure
AUT	Antenna under test
BW	Bandwidth
CATR	Compact antenna test range
CCDF	Complementary cumulative distribution function
CDF	Cumulative distribution function
DFF	Direct far field
EBW	Emission bandwidth
EIRP	Equivalent isotropic radiated power
EIS	Equivalent isotropic sensitivity
EVM	Error vector magnitude
FAC	Full anechoic chamber
FF	Far field
FSPL	Free space path loss
FWA	Fixed wireless access
HPBW	Half-power beamwidth
IFF	Indirect far field
MCS	Modulation and coding scheme
MU	Measurement uncertainties
NF	Near field
NF	Noise figure
OBW	Occupied bandwidth
OOBE	Out-of-band emissions
OTA	Over the air
PDF	Probability distribution function
QCL	Quasi co-location
QZ	Quiet zone
RMC	Reference measurement channel
RMS	Root mean square
RSRP	Reference signal receive power
SEM	Spectrum emission mask
SS-RSRPB	Synchronization signal reference signal received power per branch
TIS	Total isotropic sensitivity
TRP	Total radiated power
UBF	UE beamlock function
UE	User equipment
VSWR	Voltage standing wave ratio

Rohde & Schwarz

The Rohde & Schwarz electronics group offers innovative solutions in the following business fields: test and measurement, broadcast and media, secure communications, cybersecurity, monitoring and network testing. Founded more than 80 years ago, the independent company which is headquartered in Munich, Germany, has an extensive sales and service network with locations in more than 70 countries.

www.rohde-schwarz.com

Rohde & Schwarz customer support

www.rohde-schwarz.com/support

PD 3609.5897.52 | Version 01.00 | April 2021 (ch) | White paper
Over-the-air RF conformance measurements on 5G NR devices
Data without tolerance limits is not binding | Subject to change

3609588752
3609.5897.52 01.00 PDP/PDW 1 en